Article

Cell Reports

TREX1 Knockdown Induces an Interferon Response to HIV that Delays Viral Infection in Humanized Mice

Graphical Abstract

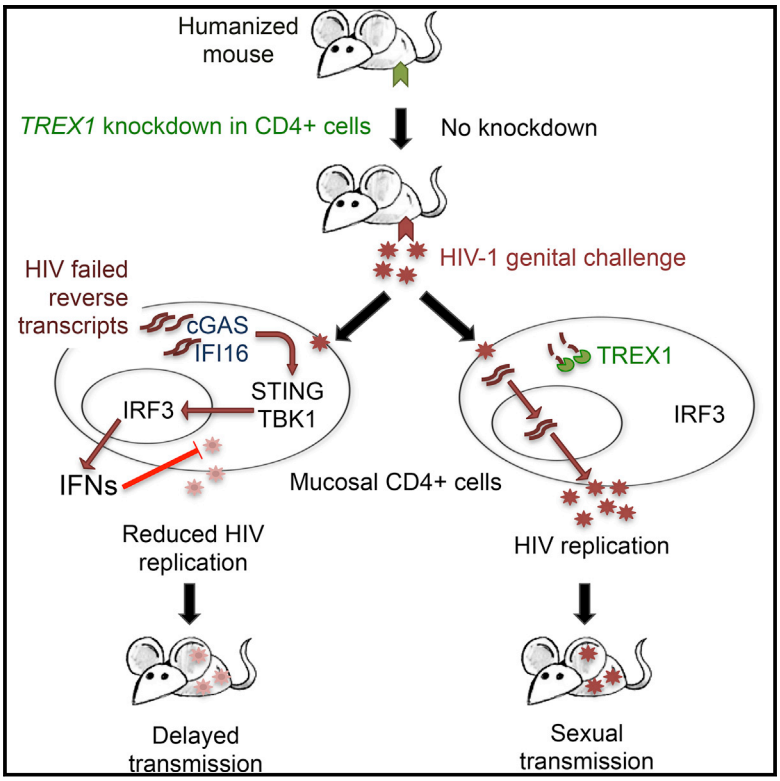

Highlights

- CD4-aptamer-siRNA chimeras knock down *TREX1* in $CD4^+$ cells in the genital mucosa
- Knocking down *TREX1* increases type I IFN production by HIV-infected mucosal cells
- *TREX1* knockdown in genital mucosa suppresses HIV infection through IFN induction
- *TREX1* knockdown in the genital tract delays HIV transmission in vivo

Authors

Lee Adam Wheeler, Radiana T. Trifonova, Vladimir Vrbanac, ..., Andrew D. Luster, Andrew M. Tager, Judy Lieberman

Correspondence

judy.lieberman@childrens.harvard.edu

In Brief

Wheeler et al. describe the effect of knocking down *TREX1* on genital HIV transmission in humanized female mice. Knocking down *TREX1* in mucosal $CD4^+$ cells using CD4-aptamer-siRNA chimeras increases type I IFN production by HIV-infected cells and delays HIV infection.

Wheeler et al., 2016, Cell Reports *15*, 1715–1727
May 24, 2016
http://dx.doi.org/10.1016/j.celrep.2016.04.048

Cell Reports
Article

TREX1 Knockdown Induces an Interferon Response to HIV that Delays Viral Infection in Humanized Mice

Lee Adam Wheeler,[1,2,4] Radiana T. Trifonova,[1,4] Vladimir Vrbanac,[3] Natasha S. Barteneva,[1] Xing Liu,[1] Brooke Bollman,[1] Lauren Onofrey,[1] Sachin Mulik,[1] Shahin Ranjbar,[1] Andrew D. Luster,[3] Andrew M. Tager,[3] and Judy Lieberman[1,*]

[1]Program in Cellular and Molecular Medicine, Boston Children's Hospital and Department of Pediatrics, Harvard Medical School, Boston, MA 02115, USA

[2]MD-PhD Program, Harvard Medical School, Boston, MA 02115, USA

[3]Center for Immunology and Inflammatory Diseases, Massachusetts General Hospital, Harvard Medical School, Boston, MA 02139, USA

[4]Co-first author

*Correspondence: judy.lieberman@childrens.harvard.edu

http://dx.doi.org/10.1016/j.celrep.2016.04.048

SUMMARY

Despite their antiviral effect, the in vivo effect of interferons on HIV transmission is difficult to predict, because interferons also activate and recruit HIV-susceptible cells to sites of infection. HIV does not normally induce type I interferons in infected cells, but does if *TREX1* is knocked down. Here, we investigated the effect of topical *TREX1* knockdown and local interferon production on HIV transmission in human cervicovaginal explants and humanized mice. In explants in which *TREX1* was knocked down, HIV induced interferons, which blocked infection. In humanized mice, even though *TREX1* knockdown increased infiltrating immune cells, it delayed viral replication for 3–4 weeks. Similarly intravaginal application of type I interferons the day before HIV infection induced interferon responsive genes, reduced inflammation, and decreased viral replication. However, intravenous interferon enhanced inflammation and infection. Thus, in models of human sexual transmission, a localized interferon response inhibits HIV transmission but systemic interferons do not.

INTRODUCTION

Most viruses trigger expression of type I interferons (IFNs) when pattern recognition receptors detect viral nucleic acids (Coccia et al., 1994). IFNs orchestrate comprehensive antiviral gene expression programs within infected cells and promote innate and acquired antiviral immune responses by enhancing antigen recognition, lymphocyte activation, and recruitment of immune cells to infection sites. Acute infection with the HIV, however, does not induce antiviral IFNs in the $CD4^+$ T cells and macrophages that are productively infected (Goldfeld et al., 1991; Unterholzner and Bowie, 2008; Yan et al., 2010). HIV evades immune surveillance at multiple stages of the viral life cycle. During viral entry, Toll-like receptor (TLR) RNA sensors do not recognize HIV genomic RNA, because most virions bypass endosomes where these sensors are located. After fusion, genomic RNA is shielded within the viral capsid from cytosolic RNA receptors. HIV reverse transcripts are bound at both ends to HIV integrase, which is predicted to interfere with recognition by cGAS, the cytosolic DNA sensor. However, HIV reverse transcriptase (RT) also generates incomplete reverse transcripts that are not bound to integrase. These can trigger the cGAS-STING-IRF3 pathway of IFN induction if they are not digested by TREX1, a ubiquitous cytosolic 3′–5′ exonuclease (Cai et al., 2014; Gao et al., 2013; Sun et al., 2013; Yan et al., 2009, 2010). When *TREX1* is knocked down or knocked out, in vitro HIV infection triggers type I IFN expression in infected cells that inhibits viral replication. Type I IFNs can also be induced by mutating the HIV capsid or depleting host cofactors with which it interacts and by knocking down *SAMHD1* (Lahaye et al., 2013; Rasaiyaah et al., 2013; Zhang et al., 2014).

Although IFNs have a strong and unequivocal antiviral effect for most viruses, because HIV infects immune cells, the net effect of IFNs on HIV is more complicated. Type I IFNs block both early and late stages of the HIV life cycle (Agy et al., 1995; Coccia et al., 1994; Shirazi and Pitha, 1992). Although type I IFNs also induce the expression of all known HIV restriction factors, including the APOBECs, SAMHD1, and tetherin, type I IFNs can potentially enhance HIV infection by promoting T cell activation and recruiting HIV-susceptible cells to the site of infection. Therefore, although in vitro experiments show that TREX1 deficiency inhibits HIV replication, the in vivo consequences of *TREX1* knockdown are difficult to predict.

The antiviral effects of type I IFNs prompted researchers to evaluate their administration as a treatment of HIV infection in the early days of the HIV epidemic. Early studies showed clinical improvement (Hübner et al., 2007; Judge et al., 2005). These promising results were replicated by two randomized control studies, which demonstrated that IFNα treatment significantly reduced viral loads in chronically infected patients (Jackson et al., 2006; Saba et al., 2010). However, subsequent clinical trials did not demonstrate similar therapeutic benefit (Fitzgerald-Bocarsly and Jacobs, 2010; Lehmann et al., 2010; Swiecki and Colonna, 2010). Researchers abandoned IFN-based therapies

when highly active antiretroviral therapy (HAART) became widely available in the mid-1990s (Saba et al., 2010; Wu and KewalRamani, 2006). IFNs, like other cytokines, are meant to act locally at the site of infection and are probably most effective at controlling viral infection when they are produced at high concentrations where the infection begins. The high concentrations required for therapeutic benefit when exogenous IFN is administered lead to systemic side effects, including fever, neutropenia, and depression. The equivocal outcomes of systemic IFN treatment may have been due, in part, to the nonspecific generalized immune activation that accompanies sustained systemic IFN administration. Knocking down *TREX1* does not induce IFNs in uninfected cells (Yan et al., 2010), providing a means to localize IFN production to infected cells and evaluate whether IFNs produced in infected cells provide a net protective effect.

Here, we knock down *TREX1* using CD4-aptamer-small interfering RNA (siRNA) chimeras (CD4-AsiCs) in $CD4^+$ cells in human cervicovaginal explants and in the genital tract of female humanized mice to evaluate the effect on HIV transmission of localized IFN production in infected cells. We previously showed that CD4-AsiCs, which are composed of a CD4-targeting aptamer covalently linked to the passenger strand of an siRNA and then annealed to the active strand, cause specific gene knockdown in $CD4^+$ T cells and monocytes/macrophages without toxicity, cell activation, or innate immune off-target effects (Wheeler et al., 2011, 2013). Gene knockdown in tissue lasts for almost 2 weeks (Collins et al., 2000; Wheeler et al., 2011). Topical application of CD4-AsiCs designed to knock down *CCR5* and/or HIV *gag* and *vif* block vaginal transmission in humanized mice.

Because studying early events in the sexual transmission of HIV in humans is difficult, our understanding of sexual transmission of the virus relies heavily on studies in macaques challenged with cell-free simian immunodeficiency virus (SIV) (Arfi et al., 2008; Bergamaschi and Pancino, 2010; d'Ettorre et al., 2014; Miller et al., 2005; Piguet and Steinman, 2007). In this model, SIV first infects and expands in $CD4^+$ T cells in the genital mucosa before spreading to myeloid cells (Haase, 2010; Miller et al., 2005; Zhang et al., 1999). Infection is contained within the genital tract for ~1 week before disseminating to regional lymph nodes and systemically. This provides a "window of opportunity" for interventions to prevent HIV from establishing a foothold. Genital infection stimulates a pro-inflammatory cytokine cascade, which recruits activated immune cells to the genital mucosa (Caux et al., 2000; Dieu-Nosjean et al., 1999; Miller et al., 2005), which then promotes viral replication and spreading, both locally and systemically. Plasmacytoid dendritic cells (pDCs), the primary producers of type I IFNs, are recruited to the genital mucosa, but IFN production is delayed (Klatt et al., 2014). Thus, because SIV does not induce IFNs in infected cells and IFN production by recruited cells in the genital tract is delayed, SIV does not have to cope with the antiviral effects of host IFNs while it is establishing the infection.

A recent study investigated the effect of manipulating type I IFNs on transmission of repeated SIV rectal challenges in rhesus macaques (Sandler et al., 2014). Blocking the type I IFN receptor increased viral replication and AIDS progression, while administration of IFN-α2a around the time of challenge blocked transmission. However, continued exposure to exogenous IFNs actually caused desensitization to its antiviral effect, increased the viral setpoint, and accelerated disease progression. This work highlights the potential protective role of type I IFNs but also suggests that the in vivo effects of IFNs are complex.

Immune responses can differ between human and nonhuman primates, since immune genes continue to coevolve with pathogens, and SIV differs in important ways from HIV. In particular, the SIV viral protein Vpx promotes degradation of host restriction factor SAMHD1, which limits HIV infection in resting T cells and myeloid cells, thereby enabling SIV to replicate in cell populations that HIV cannot. Given the complexity of the effects of IFNs, which activate components of the immune system capable of both propagating and inhibiting HIV (Boasso et al., 2008; Fitzgerald-Bocarsly and Jacobs, 2010; Hardy et al., 2009; Poli et al., 1994), it is important to study the role of IFNs in HIV transmission in human systems. In particular, the exact role IFNs play in acute HIV infection, the timing of their induction, and the effects they exert on their most immediate downstream targets during the earliest stages of viral transmission remain poorly understood. Here, we use two HIV-human transmission model systems, polarized human cervicovaginal explants and humanized mice, to investigate the effect of inducing type I IFNs in infected cells by *TREX1* knockdown to assess the effects of endogenous IFNs on HIV female genital transmission. These models both have limitations. The explants are only viable for 10–14 days (Collins et al., 2000; Wheeler et al., 2011) and do not take into account recruitment of immune cells to the tissue. Although human myeloid and lymphoid cells are present in the female genital tract of humanized mice, they are less abundant than in human tissues, and their lymph nodes are often undeveloped or absent (Olesen et al., 2011). Moreover, humanized mice have chronic immune activation from graft versus host responses. Although there is good cross-reactivity between human and mouse cytokines and chemokines, signaling may not replicate precisely what occurs in humans. Nonetheless, these imperfect models are as close as we can get to human transmission.

Here, we show that CD4-AsiCs knock down *TREX1* expression by 75%–95% in human cervicovaginal tissue and the female genital tract of humanized mice. Knocking down *TREX1* increased expression of type I IFNs and interferon-stimulated genes (ISGs) in HIV-exposed, but not uninfected, human tissue and humanized mice in the first 12–24 hr after exposure, but did not cause upregulation of inflammatory cytokines, such as IL1β, IL-6, and IL-8. Intravaginal (IVAG) IFN administration had a similar effect. In contrast, exogenous IFNs, given intravenously (i.v.) to humanized mice, induced ISGs as well as proinflammatory cytokine gene expression, even in the absence of HIV infection. In tissue explants, *TREX1* knockdown suppressed HIV infection, and suppression was largely mediated by type I IFNs, since it was strongly inhibited by neutralizing antibodies to type I IFNs. In humanized mice, a robust type I IFN response decreased viral replication during the first 48 hr after exposure, despite recruitment of immune cells to the genital mucosa. Importantly, *TREX1* knockdown in the genital tract delayed HIV infection for ~3–4 weeks, suggesting that IFN induction in infected cells suppresses local viral replication.

RESULTS

TREX1 Knockdown in CD4$^+$ Cells In Vitro and in Human Cervicovaginal Tissue Explants

CD4-AsiCs were designed to knock down *TREX1* in CD4$^+$ cells using the CD4 aptamer and siRNA linkage, previously shown to knock down *CCR5* and viral genes selectively in CD4$^+$ T cells and macrophages in cervicovaginal tissue explants and the genital tract of humanized mice (Wheeler et al., 2011, 2013). The aptamer directs the chimeric RNA selectively into CD4$^+$ cells, where Dicer cleaves the AsiC to separate the aptamer from the siRNA. A chimeric RNA encoding the CD4 aptamer linked at its 3′-end to the sense strand of one of two *TREX1* siRNAs was in vitro transcribed using 2′-fluoropyrimidines to enhance stability and minimize off-target effects (Figures 1A and 1B). The in vitro transcribed RNA was then annealed to the antisense siRNA strand. To evaluate gene knockdown, peripheral blood mononuclear cells (PBMCs) were incubated for 48 hr with 0.25–4 μM *TREX1* CD4-AsiCs and analyzed by qRT-PCR for *TREX1* mRNA (Figures 1C and 1D). *TREX1* knockdown occurred specifically in CD4$^+$, but not CD8$^+$ T cells. The best knockdown occurred using 4 μM AsiC. "Sequence a," which knocked down *TREX1* by ~50% even at the lowest concentration and by ~90% at the highest concentration, was more effective than "sequence b" and was used for subsequent experiments, unless otherwise noted. *TREX1* knockdown in primary human CD4$^+$ T cells also significantly reduced TREX1 protein and the proportion of cells that stained above background for TREX1 from 83% to 7%, as assessed by flow cytometry (Figure S1).

Type I IFN signaling leads to phosphorylation and nuclear translocation of the IRF3 transcription factor. To investigate whether IFN signaling is activated after HIV infection in cells knocked down for *TREX1*, we assessed IRF3 localization by imaging flow cytometry in primary human monocyte-derived macrophages (MDMs) and CD4$^+$ T cells (Figures S2A and S2E). *TREX1* knockdown did not significantly change IRF3 localization in uninfected cells. However, as expected, IRF3 translocated to the nucleus after HIV infection in cells knocked down with *TREX1* siRNA compared to cells transfected with a non-targeting negative control siRNA (MDMs, $p < 0.01$; CD4$^+$ T cells, $p < 0.0001$). To determine whether IRF3 activation is mediated by cGAS and IFI16, DNA sensors that recognize HIV reverse transcripts (Gao et al., 2013; Monroe et al., 2014), we co-transfected CD4$^+$ T cells with *TREX1* siRNA alone or together with *cGAS* or *IFI16* siRNAs. siRNA targeting the DNA sensor AIM2 or the RNA sensor RIG-I, which are not required for the induction of type I IFN by HIV in TREX1 knockout cells (Yan et al., 2010), were used as controls. Knockdown of *cGAS* or *IFI16*, but not *AIM2* or *DDX58*, the gene encoding RIG-I, significantly and strongly inhibited IRF3 nuclear translocation in response to HIV infection in *TREX1* knocked down cells (Figures S2F–S2K). Thus, *TREX1* knockdown induces IFN pathway activation and IRF3 nuclear translocation in response to HIV that is dependent on DNA sensing by both cGAS and IFI16, like recognition of HSV-1 and Listeria monocytogenes DNA (Orzalli et al., 2015; Hansen et al., 2014).

Next, we evaluated *TREX1* gene knockdown in human cervicovaginal explants. *TREX1* CD4-AsiCs (1 and 4 μM) were applied twice at an interval of 24 hr to the epithelial surface of polarized human cervicovaginal tissue. Four days after the second treatment, tissues were digested to single cell suspensions, which were sorted into CD4$^+$/CD3$^+$ T cells, CD4$^+$/CD14$^+$ macrophages, and CD19$^+$ B cell subsets and analyzed for *TREX1* mRNA by qRT-PCR (Figures 1E and 1F). *TREX1* was knocked down by 80%–95% in CD4$^+$ T cells and macrophages, but not in B cells. Both concentrations led to comparable knockdown. We previously showed that CD4-AsiCs targeting other genes do not activate an innate immune IFN response on their own (Wheeler et al., 2011). However, because IFN induction may be sequence-dependent, we evaluated whether *TREX1*-specific CD4-AsiCs induce type I IFNs. We treated cervical explants with *TREX1* CD4-AsiCs in the absence of HIV infection and measured expression levels of type I IFN mRNAs in the tissue at the expected peak response time (6 hr) by sensitive qRT-PCR assay (Figure S3A). As expected, *TREX1* CD4-AsiCs did not induce an IFN response, whereas Poly(I:C), used as a positive control, did.

TREX1 Knockdown Inhibits HIV Replication and Induces IFN-β in Polarized Human Cervicovaginal Explants

TREX1 knockdown inhibits HIV expression in vitro by upregulating type I IFNs (Yan et al., 2010). To evaluate whether knocking down *TREX1* also inhibits HIV infection in human tissue, we used a previously validated polarized human cervicovaginal explant model of HIV transmission and infection. The observed p24 Ag production in infected explants measured active viral replication in the explants, rather than carryover of virus in the infectious inoculum, since p24 Ag levels did not increase in tissues that were infected in the presence of the HIV inhibitors, AZT, or nevirapine (Figure S3B). To evaluate the effect of *TREX1* knockdown in the explant system, we measured viral replication in cervicovaginal tissue from three healthy donors infected after they were treated with PBS or CD4-AsiCs against *TREX1* or, as positive control, a cocktail against *CCR5*, *gag*, and *vif*. Explants were treated 3 and 2 days prior to challenge with HIV_{BaL}, and viral replication was monitored by measuring viral p24 antigen in the lower Transwell chamber (Figures 2A–2C). As previously demonstrated, the *CCR5* and antiviral gene cocktail completely prevented productive HIV infection. CD4-AsiCs encoding either *TREX1* siRNA sequence inhibited HIV infection, but "sequence a" performed better, almost completely suppressing p24 Ag production. Although HIV infection in the absence of gene knockdown did not lead to detectable IFNβ release until day 9 of culture, when it was barely above background, the infected tissues that were treated with *TREX1* AsiCs produced IFNβ that was detected in the first measurement on day 3 (Figure 2D). Tissues treated with the more effective "sequence a" AsiC generated more IFNβ. Tissues treated with the CD4-AsiC cocktail that blocked infection did not release IFNβ. To evaluate the importance of type I IFNs in inhibiting HIV transmission in the tissue, blocking monoclonal antibodies (mAbs) to IFNα and IFNβ were added to the culture medium 24 hr before and at the time of infection (Figures 2E–2G). The blocking antibodies had no effect on HIV production in explants that were knocked down for *CCR5* and the viral genes, which was not surprising since they did not generate type I IFNs. Antibody treatment blunted the amount of

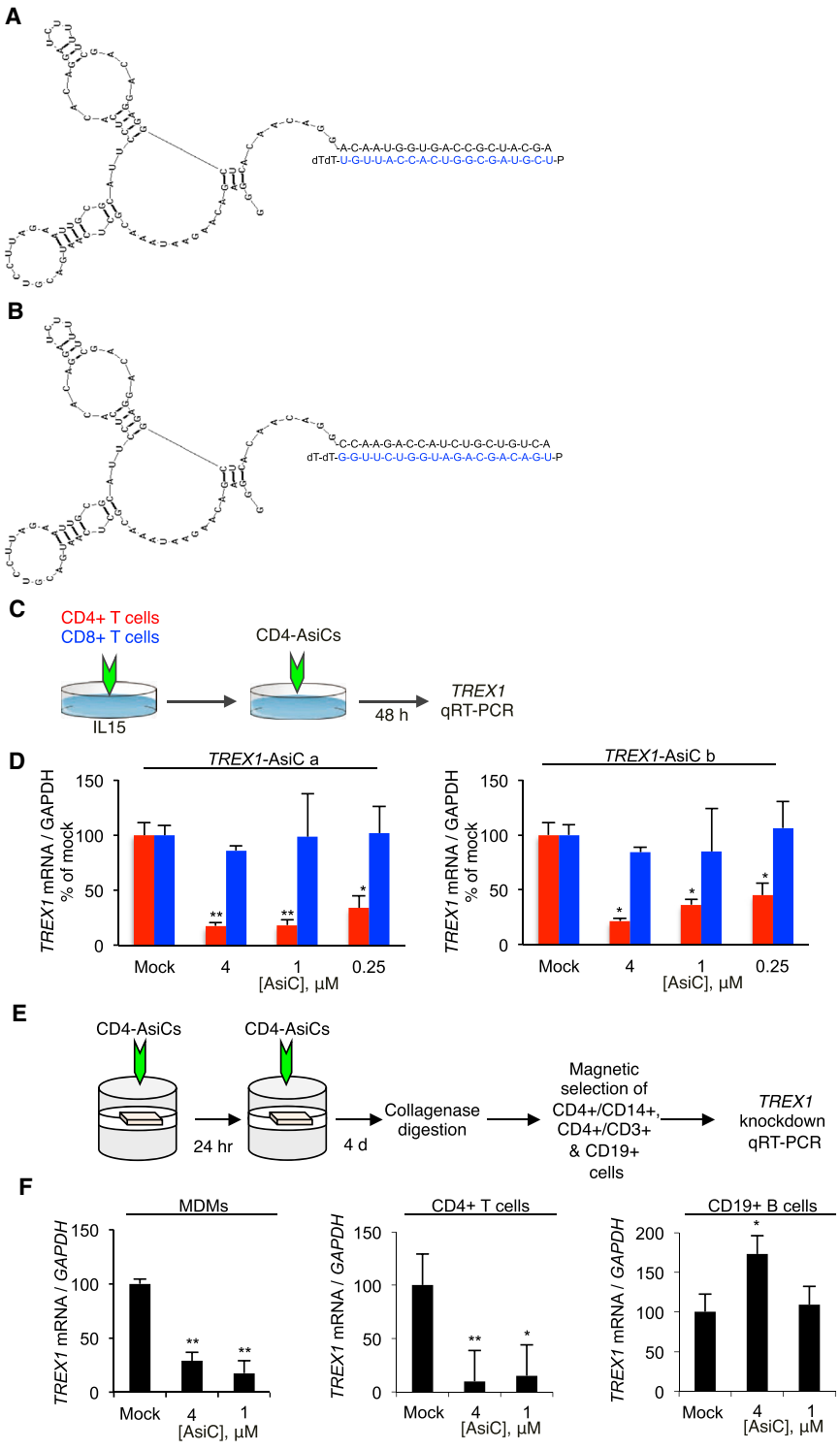

Figure 1. CD4-AsiCs Knockdown *TREX1* in CD4$^+$ Cells In Vitro and in Polarized Cervicovaginal Explants

(A and B) Two *TREX1* CD4-AsiCs (sequence a, A; sequence b, B).

(C and D) CD4$^+$ (red) and CD8$^+$ (blue) T cells were treated and analyzed for *TREX1* gene knockdown by qRT-PCR relative to *GAPDH*. Experimental schematic in (C). Relative *TREX1* knockdown after application of *TREX1* CD4-AsiC sequence a (left) and sequence b (right) is shown (D).

(E and F) CD4$^+$CD14$^+$ monocyte-derived macrophages (MDMs), CD4$^+$ T cells, and CD19$^+$ B cells, sorted from polarized cervicovaginal explants treated with *TREX1* CD4-AsiCs, or PBS (mock), were analyzed for *TREX1* knockdown by qRT-PCR. Graphs show mean ± SEM from three independent experiments. *$p < 0.05$, **$p < 0.005$, ***$p < 0.0005$, by Student's t test, relative to mock-treated control samples. The change in *TREX1* in B cells was not reproducible. Experimental schematic in (E). Relative TREX1 knockdown 4 d after application of TREX1 CD4-AsiC sequence a or PBS to MDMs (left), CD4+ T cells (middle) or CD19+ B cells (right) is shown (F).

See also Figure S1.

IFNβ protein detected in the culture supernatants and increased HIV infection in *TREX1* AsiC-treated explants. However, blocking IFNα and IFNβ in *TREX1* AsiC-treated tissues did not completely restore HIV infection to the level observed in tissues not subjected to knockdown. Thus, *TREX1* knockdown suppressed HIV infection in cervicovaginal tissues, largely via induction of type I IFNs.

Recently transmitted HIV-1 viruses, termed transmitted/founder (T/F) viruses, are relatively resistant to suppression by type I IFNs (Parrish et al., 2013). To determine whether *TREX1* knockdown could inhibit infection with T/F HIV-1 virus, we compared the effect of *TREX1* knockdown on replication of a T/F virus relative to HIV$_{BaL}$ in human cervical explants (Figure S4), using treatment with the CD4 aptamer on its own as a control. T/F HIV replication was significantly inhibited by treatment with *TREX1* CD4-AsiCs. However, T/F virus was less strongly suppressed than HIV$_{BaL}$.

Exposure of MDMs to Type I IFN Inhibits HIV Replication when Administered Just before or after Infection

To prepare for in vivo experiments with IFNs, we first defined the dose-dependence and timing of IFN protection from HIV infection in vitro. MDMs were incubated for 24 hr with different amounts of a recombinant form of IFN, engineered to bind multiple IFN receptors with high affinity (rIFN), prior to infection with three doses of HIV$_{BaL}$ (Figure S5). Adding 10,000 IU recombinant interferon (rIFN) in 0.3 ml culture medium suppressed viral replication in MDMs by >95% for even the highest viral challenge. At the

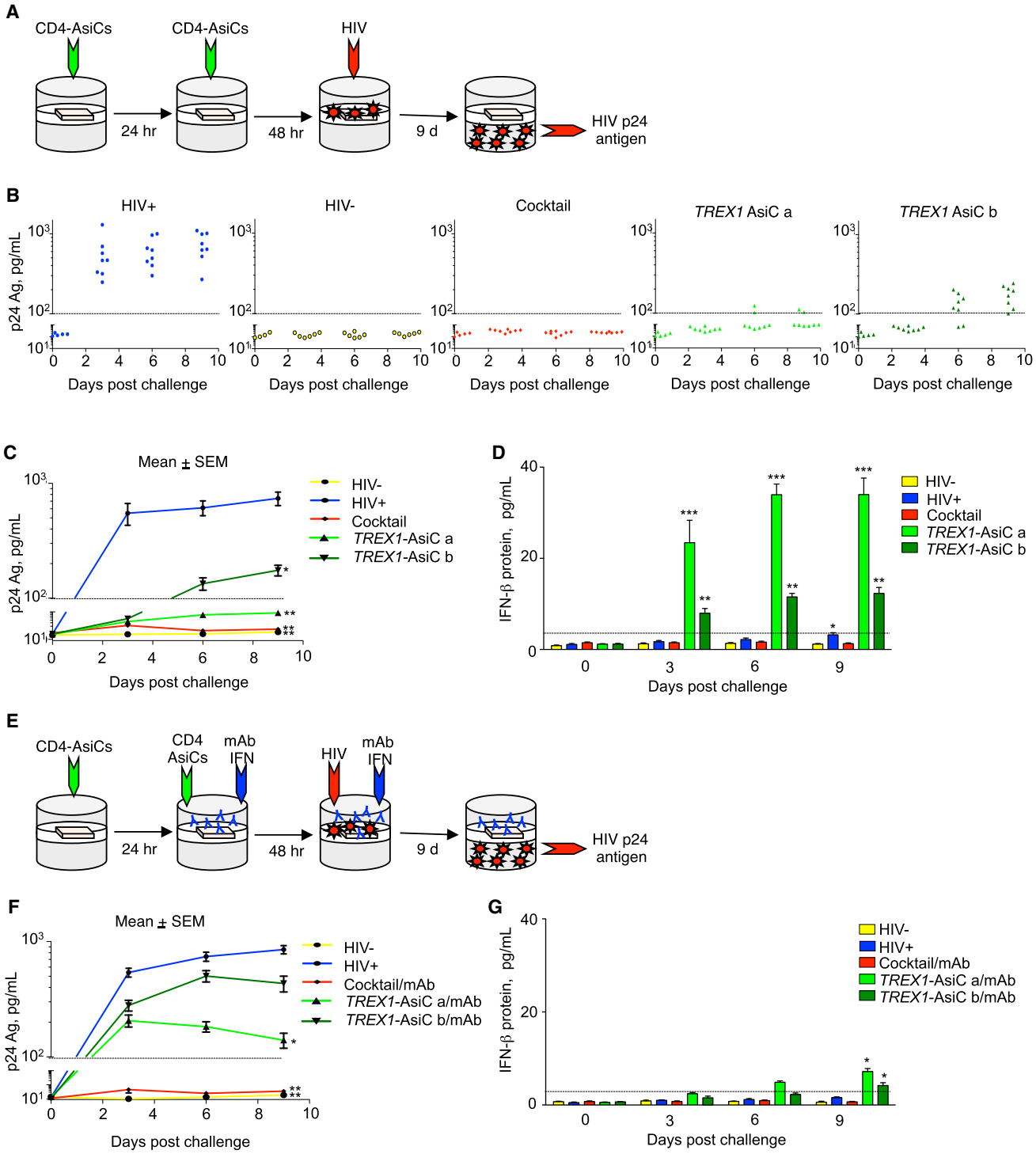

Figure 2. CD4-AsiC Knockdown of *TREX1* Inhibits HIV Replication in Polarized Human Cervicovaginal Explants Partly by Inducing Type I IFNs

(A–D) Polarized explants (n = 8) from three donors treated with PBS (blue) or twice pretreated with 4 μM CD4-AsiCs targeting *TREX1* (siRNA sequence a, light green; siRNA sequence b, dark green) or *CCR5*, *gag*, and *vif* (cocktail, red) before HIV-1_{BaL} challenge. Data for uninfected control cultures are shown in yellow. Experimental schematic in (A). HIV infection analyzed by p24 Ag ELISA (B and C) and IFN-β protein measured by ELISA (D).

(E–G) Blocking monoclonal antibodies (mAbs) against IFN-α and IFN-β were applied 24 hr prior to and at the time of HIV challenge. Graphs show mean ± SEM. *p < 0.05, **p < 0.005, ***p < 0.0005, by Student's t test, relative to uninfected control. Experimental schematic in (E). Shown is a time course of p24 Ag (F) and IFN-β (G) protein levels in the lower chamber after HIV infection.

See also Figures S2, S3, and S4.

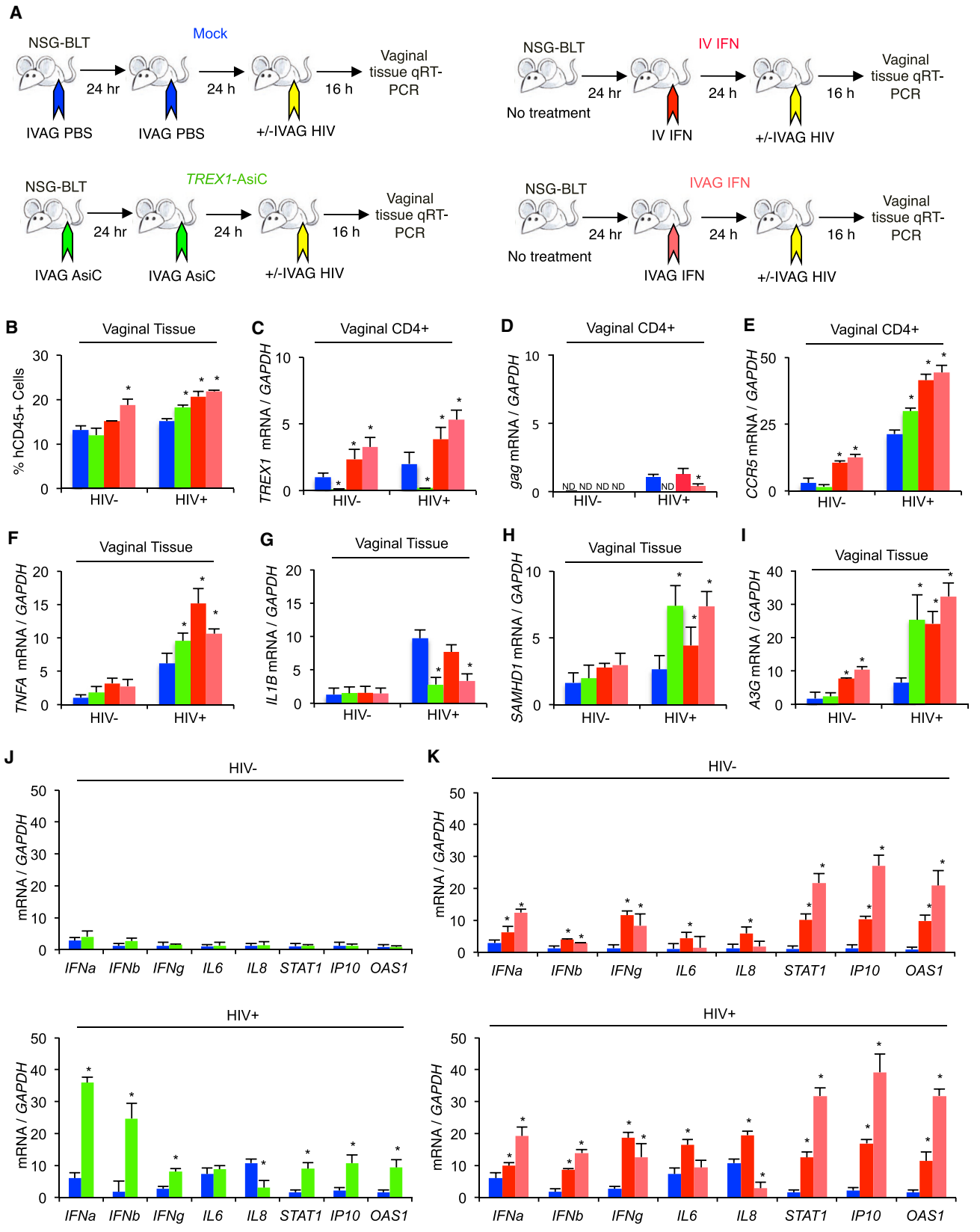

(legend on next page)

highest concentration, rIFN completely prevented viral replication when added up to 24 hr prior to or within 6 hr after viral challenge. At the lower doses, adding the recombinant protein 6 hr before infection was more effective than adding it 24 hr before infection. When rIFN was added 2 days before or 1 day after viral challenge, there was little protection.

TREX1 Knockdown IVAG or Topical rIFN Upregulate ISGs and Inhibit Early HIV Replication in Humanized BLT Mice

To investigate the in vivo effect of *TREX1* expression on HIV transmission, we treated humanized BLT mice IVAG with PBS or 40 pmol of *TREX1* CD4-AsiCs on 2 consecutive days. Half of the mice were not exposed to HIV and half were challenged the following day with $HIV1_{JR-CSF}$ using a viral dose that reproducibly infects all control mice (n = 6) (Wheeler et al., 2011, 2013) (Figure 3A). Additional groups of mice (n = 6) were treated with i.v. rIFN (10^4 IU) or IVAG rIFN (2×10^3 IU) the day before viral challenge. One hour post-rIFN administration, we measured rIFN levels in the serum. After i.v. injection, rIFN was detected in the serum at a level of 43.5 ± 0.57 IU/ml (n = 3), but it was not detectable in the serum after IVAG application (data not shown). Mice were sacrificed 16 hr after viral challenge, and cervicovaginal tissue was digested into single cell suspensions. Systemic IFN significantly increased the number of human $CD45^+$ hematopoietic cells in the female genital tract, irrespective of HIV infection, while *TREX1* knockdown and topical IVAG IFN increased human infiltrating cells in the genital tract only following HIV infection (Figure 3B). Gene expression was examined in human $CD45^+$ hematopoietic cells, human $CD4^+$ cells, and in the total mixed cell population isolated from the vaginal mucosa by qRT-PCR. *TREX1* CD4-AsiCs strongly knocked down *TREX1* mRNA (by ~95%) in genital tract $CD4^+$ cells in both HIV uninfected and infected mice (Figure 3C). Both topical and systemic IFNs significantly increased *CCR5* and IFN-responsive *TREX1* and *APOBEC3G* and other ISG mRNAs in tissue $CD4^+$ cells (Figures 3C, 3H, 3I and 3K). In the absence of HIV infection, *TREX1* knockdown did not significantly change expression of inflammatory cytokines, *CCR5*, type I and II IFNs, or ISGs, including *SAMHD1* and *APOBEC3G* (Figures 3E–3J).

After HIV challenge, HIV *gag* mRNA was detected above background in control and IFN-treated BLT mouse genital tissue, but was not detected in mice treated with *TREX1* AsiCs at this early time point (Figure 3D). Thus, *TREX1* knockdown was protective. *TREX1* knockdown, and to a greater extent topical and systemic IFNs, also increased *CCR5* mRNA in CD4+ cells in the genital tissue, likely due to infiltration of activated immune cells and activation of tissue resident cells (Figures 3B and 3E). With exposure to HIV, *TREX1* knockdown led to significantly increased type I and type II IFNs and ISG mRNAs, including the mRNAs for the HIV restriction factor ISGs, *SAMHD1* and *APOBEC3G* (Figures 3H–3J). *TREX1* knockdown did not have a consistent effect on HIV-induced inflammatory gene expression—it significantly increased TNFα, reduced IL-1β and IL-8, and did not change IL-6 mRNA expression. Thus, early after HIV infection, *TREX1* knockdown in $CD4^+$ cells in the female genital tract reduced HIV load and induced IFNs and antiviral gene expression, but at the same time, increased recruitment of activated $CCR5^+$ immune cells, expanding the numbers of susceptible cells in the tissue.

Topical, but not systemic, IFN significantly suppressed early HIV replication, assessed by measuring *gag* mRNA 16 hr after infection, compared to control mice, but inhibition was less effective than *TREX1* knockdown, which suppressed HIV to undetectable levels (Figure 3D). Systemic rIFN more potently induced ISG expression than *TREX1* knockdown, but also enhanced tissue recruitment of $CCR5^+$ hematopoietic cells and caused more pro-inflammatory gene expression. The recruitment of activated HIV-susceptible cells and induction of inflammation in the genital tract after systemic IFN administration may have canceled the antiviral effects of ISGs on HIV replication.

TREX1 CD4-AsiCs Upregulate Gene Expression of Type I IFNs and ISGs in the Vaginal Tissue of HIV-Exposed Humanized BLT Mice

Next, we evaluated the effect of *TREX1* knockdown on gene expression in the female genital tract of humanized mice 24 and 48 hr after viral challenge (Figure 4A). Mice treated IVAG with *TREX1* AsiCs were compared to mice treated IVAG with PBS as negative control, or lipopolysaccharide (LPS), which induces both type I IFNs and inflammatory cytokines, as positive control. Each group was treated on 2 consecutive days and challenged with HIV IVAG on the following day. Blood and cervicovaginal tissue were harvested 24 and 48 hr later, single cell suspensions were prepared, and human $CD4^+$, human $CD45^+$, and total cell populations were analyzed for mRNA expression by qRT-PCR (Figures 4C–4I). IVAG LPS, as expected, increased the numbers of human $CD45^+$ cells in the vaginal tissue (Figure 4B). *TREX1* AsiCs knocked down *TREX1* in $CD4^+$ cells in the genital tract by

Figure 3. *TREX1* Knockdown or Topical IFN Upregulate ISGs and Inhibit HIV Transmission in Humanized Mice

(A) Schematic. BLT mice (n = 6 per treatment group) were treated twice IVAG with PBS (blue) or 40 pmol *TREX1* CD4-AsiCs (green) or once with rIFN 10^4 IU IV (dark red) or 2×10^3 IU IVAG (light red). Half of the mice in each group (n = 3) were challenged 24 hr after the last treatment with HIV_{JR-CSF}, and all mice were sacrificed 16 hr after that. Cervicovaginal tissue was digested to a single cell suspension and sorted into human $CD45^+$ and $CD4^+$ cell populations.

(B) Flow cytometry analysis of human $CD45^+$ cells in the vaginal tissue of each group of mice.

(C–E) RNA from sorted cells or total tissue was analyzed for mRNA levels by qRT-PCR. *TREX1* (C) and HIV *gag* (D) mRNA in vaginal $CD4^+$ cells and *CCR5* expression in vaginal $CD45^+$ cells (E) are shown. Human gene mRNA levels, relative to GAPDH mRNA, were normalized to the value in the HIV-uninfected, PBS control. *gag* RNA, which was not detected (ND) in uninfected samples, was normalized to *GAPDH* mRNA. Shown are the mean ± SEM for each group. *$p < 0.05$ by two sided Student's t test relative to PBS control. The graphs represent data from one experiment with BLT mice prepared with human hematopoietic stem cells from one donor.

(F–K) mRNA levels for human inflammatory cytokines *TNFA* (F) and *IL1B* (G), HIV restriction factors *SAMHD1* (H) and *APOBEC3G* (I, A3G) and a panel of IFNs and ISGs (J and K) in vaginal tissue are shown. mRNA levels, relative to GAPDH mRNA, were normalized to the value in the HIV-uninfected, PBS control. Shown are the mean ± SEM for each group. *$p < 0.05$ by two-sided Student's t test, relative to PBS control. The graphs represent data from one experiment with BLT mice prepared with human hematopoietic stem cells from one donor.

See also Figure S5.

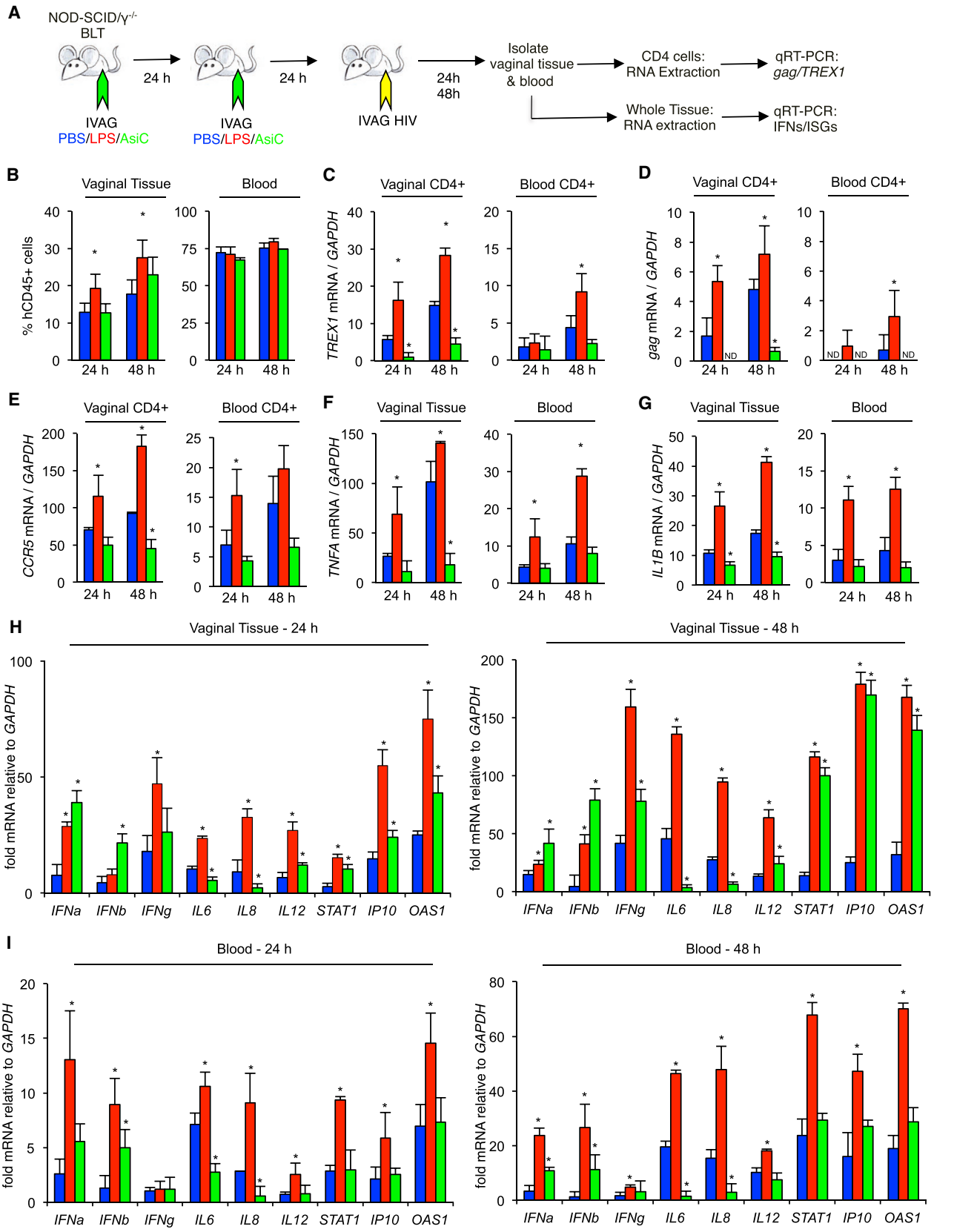

(legend on next page)

90% at 24 hr and 75% at 48 hr post challenge, while IVAG LPS significantly increased the expression of IFN-responsive *TREX1* in $CD4^+$ cells in vaginal tissue at both time points and in the blood significantly at 48 hr (Figure 4C). HIV infection in genital tract $CD4^+$ cells was suppressed to near background levels by *TREX1* knockdown at both time points, while LPS pretreatment enhanced *gag* mRNA expression in the genital tract. (Figure 4D). Unexpectedly, HIV *gag* mRNA was detected in blood $CD4^+$ cells of some LPS-treated mice at 48 hr, suggesting that infection may not be restricted to the genital tract in the setting of genital inflammation. However, because *gag* detection in blood cells was just above background, this finding needs to be interpreted with caution. *CCR5* mRNA, an indicator of T cell activation, was significantly decreased in vaginal and blood $CD4^+$ cells in *TREX1* AsiC-treated mice, while it was significantly increased in LPS-treated mice in both compartments compared to mock-treated, HIV-infected mice (Figure 4E). Knockdown of *TREX1* increased the expression of type I IFNs and ISGs and decreased expression of proinflammatory cytokines in tissue and blood, while LPS pretreatment increased both inflammation and the IFN response (Figure 4F–4I). Thus, *TREX1* knockdown in genital CD4 cells, which enhanced antiviral IFN gene expression and suppressed inflammation, blocked HIV infection at 24 hr and significantly controlled it to near background levels at 48 hr. Generalized innate immune activation by LPS administration in the genital tract enhanced HIV replication locally and accelerated dissemination.

TREX1 CD4-AsiCs Delay, but Do Not Prevent, Transmission of HIV to Humanized BLT Mice

To evaluate the net antiviral effect of *TREX1* knockdown, we compared HIV infection and $CD4^+$ T cell depletion in humanized mice treated IVAG with *TREX1* AsiCs with mock-treated mice and mice treated with the AsiC cocktail against *CCR5* and viral genes that blocks viral transmission (Wheeler et al., 2011, 2013) (Figure 5A). (The control group data were previously published in Wheeler et al. [2011], but the *TREX1* knockdown data, obtained at the same time, were not previously published.) All mock-treated mice became infected and showed profound $CD4^+$ T cell depletion (Figures 5B–5E). Viremia was first detected 3–4 weeks post-challenge, CD4 counts began to drop within 2 weeks, and $CD4^+$ T cells were severely depleted in all mice by 8 weeks. Mice treated with the cocktail were not infected—they had undetectable viremia, assessed by HIV p24 Ag and HIV gag mRNA, and no change in $CD4^+$ T cell counts. Mice treated with *TREX1* AsiCs initially looked like they were protected, but they all developed detectable viremia by 7 weeks. $CD4^+$ T cell depletion only became significant after 9 weeks. Thus, viral production was delayed for ~1 month by knocking down *TREX1* prior to viral challenge compared to control mice. Despite the delay in infection, the viral setpoint in *TREX1* AsiC-treated mice ($\sim 10^5$ copies/ml blood) and extent of $CD4^+$ T cell depletion at 12 weeks, when the experiment was terminated, were indistinguishable from those in control mice.

DISCUSSION

Here, we demonstrate that *TREX1* knockdown using CD4-AsiCs induces expression and secretion of type I IFNs and ISGs in HIV-infected cells that inhibits HIV transmission in human tissue explants and in humanized mice for several weeks when administered prior to viral challenge. Protection from HIV replication in tissue explants was largely abrogated by IFNα/β blocking antibodies, suggesting that protection is mediated by type I IFN production in infected cells. The residual protection may have been due to incomplete blockade of all type I IFNs. We also cannot exclude the possibility that some antiviral effects of *TREX1* knockdown are IFN-independent. Indeed, ISGs can be induced in the absence of TREX1 independently of IFNs (Hasan et al., 2013). Within the first 2 days after HIV challenge, HIV replication was not detected in the genital tract of mice treated with *TREX1* CD4-AsiCs and was suppressed in mice given rIFN IVAG, suggesting that local IFNs strongly inhibit HIV transmission in vivo. This was despite evidence of significant immune cell infiltration in the genital mucosa and $CD4^+$ T cell activation to express CCR5, the HIV coreceptor used during sexual transmission. In contrast, i.v. administration of rIFN using five times the IVAG dose, which induced local IFN and ISG gene expression in the genital mucosa, but less robustly than IVAG administration, did not inhibit HIV replication at this early time point. Unlike treatment with IVAG IFN or TREX1-AsiCs, i.v. IFN activated proinflammatory cytokine expression (TNFα, IL-1β, IL-6, and IL-8), which likely counteracted the protective effects provided by rIFN.

In some humanized mice (but not those treated with *TREX1* CD4-AsiCs), we detected HIV *gag* RNA at very low levels in $CD4^+$ blood cells as early as 1 and 2 days following IVAG challenge, accompanied by suggestions of systemic immune activation by qRT-PCR analysis of CCR5 and cytokine gene expression in $CD4^+$ blood cells (Figure 4D). Importantly, at these

Figure 4. *TREX1* CD4-AsiCs Upregulate Type I IFNs and ISGs and Inhibit HIV Transmission to BLT Mice

(A) Schematic. BLT mice (n = 6 per treatment group) were treated twice with IVAG PBS (blue), LPS (red), or 40 pmol *TREX1* CD4-AsiCs (green). All mice were infected with HIV_{JR-CSF}. Blood and cervicovaginal tissues were obtained at sacrifice 24 hr and 48 hr (n = 3 per treatment group) after viral challenge. PBMCs or genital tract single cell suspensions were either not sorted or sorted into human $CD45^+$ and human $CD4^+$ cell populations for analysis as indicated.

(B) Flow cytometry analysis of human $CD45^+$ cells in the tissue (left) and blood (right).

(C–E) mRNA levels relative to human *GAPDH* were analyzed by qRT-PCR for human *TREX1* (C), HIV *gag* (D), and human *CCR5* (E) using RNA extracted from $CD4^+$ cells in genital tract (left) and blood (right). Human gene mRNA levels were normalized to the value in the HIV-uninfected, PBS control. *gag* RNA was normalized to *GAPDH*. ND, not detected. All graphs show mean ± SEM. *$p < 0.05$ relative to PBS-treated control mice determined with a Student's t test. Graphs represent data from one experiment using BLT mice prepared with human hematopoietic stem cells from one donor.

(F–I) mRNA levels were analyzed by qRT-PCR on RNA extracted from genital tract single cell suspensions or PBMCs as indicated for the following human genes—*TNFA* (F), *IL1B* (G), and a panel of IFNs, inflammatory cytokines, and ISGs (H and I). mRNA levels were normalized to the value in the HIV-uninfected, PBS control. All graphs show mean ± SEM. *$p < 0.05$ relative to PBS-treated control mice, determined using Student's t test. Graphs represent data from one experiment using BLT mice prepared with human hematopoietic stem cells from one donor.

See also Figure S5.

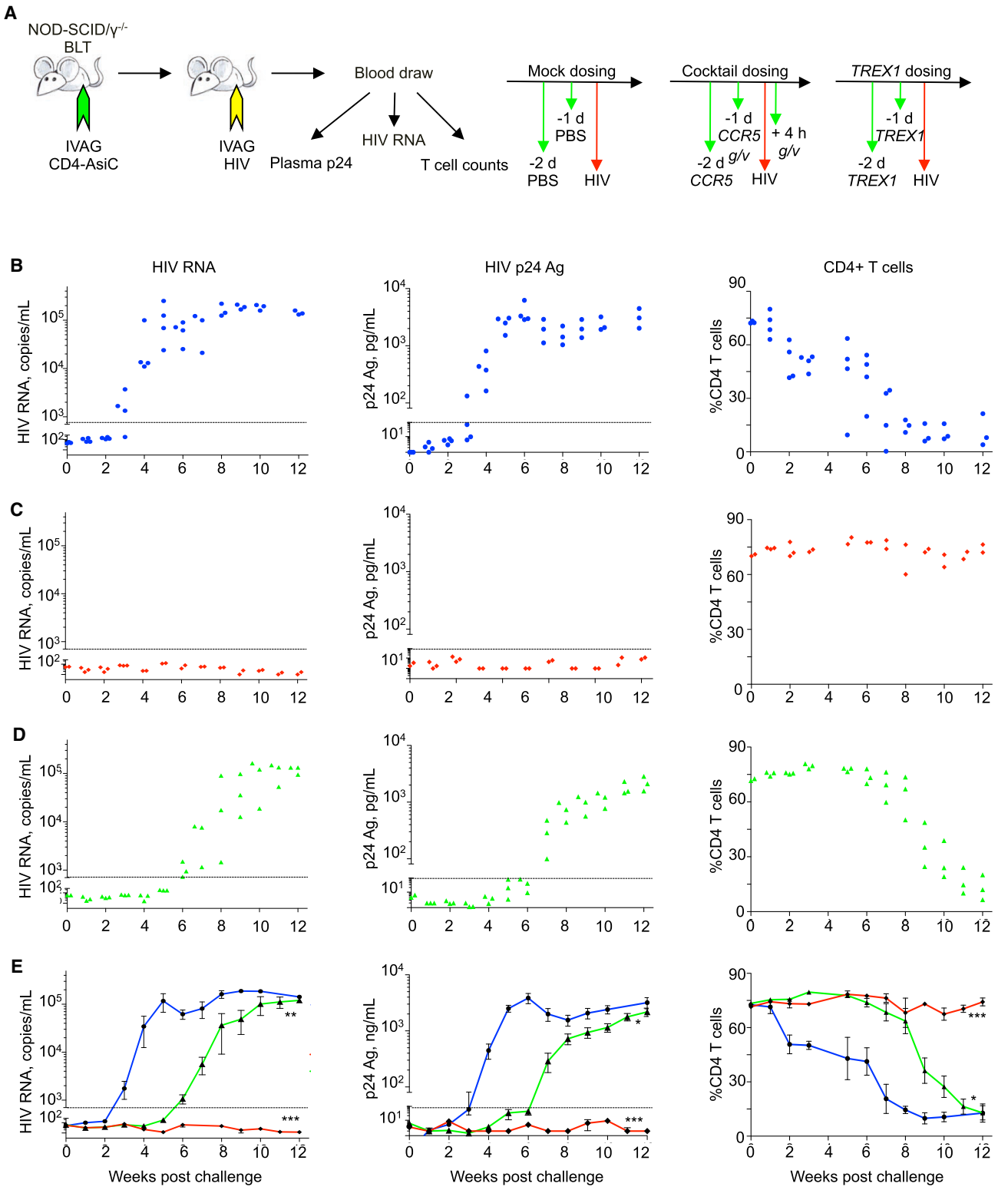

Figure 5. *TREX1* CD4-AsiCs Delay HIV Transmission to BLT Mice

(A–D) Experimental design indicated in schematic in (A). Mice (n = 4 per treatment group) were treated according to the indicated dosing schedules (right) with PBS (blue, B), a cocktail of CD4-AsiCs targeting *CCR5*, *gag* and *vif*, using a regimen that previously blocked HIV transmission (red, C) (Wheeler et al., 2011), or *TREX1* CD4-AsiCs (green, D). A total of 40 pmol of each CD4-AsiC was administered IVAG twice according to the dosing schedule. Mice were assessed for HIV

(legend continued on next page)

early times, systemic dissemination was exacerbated by IVAG pretreatment with LPS, which caused both local and systemic IFN induction and immune activation. A similar increase in sexual transmission was observed when rhesus macaques treated IVAG with other TLR agonists were challenged with SIV (Wang et al., 2005). In that case as well, both IFNs and inflammatory cytokines were induced in the genital tract. However, infected cells were not detected in the blood of mice treated IVAG with CD4-AsiCs against *TREX1*. These data suggest that in humanized mice, HIV may not be contained within the genital tract for the first week after exposure. Nonetheless, we did not detect plasma viremia by RT-PCR or p24 Ag assay until 3 weeks after infection (Figure 5). Because the level of *gag* mRNA in circulating $CD4^+$ T cells was just above background, the measured *gag* mRNA in circulating $CD4^+$ T cells within the first few days after infection should be interpreted with caution and needs to be confirmed. The discrepancy between RT-PCR analysis of $CD4^+$ T cells and plasma viremia assays suggests that RT-PCR analysis of circulating $CD4^+$ T cells may be a more sensitive way to detect systemic dissemination than amplification of viral RNA in circulating virions in the serum. Early dissemination might be the consequence of chronic low levels of immune activation from graft versus host responses that are not completely suppressed in the NOD/SCID/*Il2rg*$^{-/-}$ (NSG) mice. Their chronic immune activation may mean that conclusions about transmission in humanized mice may not reflect transmission in women, who have no underlying immune activation or vaginal coinfection. However, these mice may be a good model for women with vaginal infections, such as bacterial vaginosis or trichomonas infection, who are more vulnerable to becoming infected. If these mouse findings are confirmed, they suggest that it is worth investigating whether early viral dissemination might occur in women with ongoing vaginal or systemic infection.

Although *TREX1* knockdown suppressed HIV infection early on, HIV was transmitted with a delay in viral kinetics of ~3–4 weeks. In these experiments, *TREX1* CD4-AsiCs were administered 1 and 2 days before viral challenge. In an earlier study (Wheeler et al., 2013), *CCR5* knockdown in humanized mice using CD4-AsiCs provided complete protection from transmission when HIV challenge occurred within a day of AsiC application, but although gene knockdown in the tissue persisted for ~2 weeks, protection was incomplete when HIV challenge was delayed for 4 or 6 days. The lack of complete protection after delayed challenge was attributed to influx of HIV-susceptible cells, not exposed to AsiCs, into the genital mucosa. Similarly, in this study, HIV might have persisted in the tissue (possibly within myeloid cells that do not necessarily replicate the virus, but efficiently transmit it to T cells) (Arfi et al., 2008; Bergamaschi and Pancino, 2010; Kumar et al., 2014; Piguet and Steinman, 2007) and then replicated in tissue resident $CD4^+$ cells in which *TREX1* knockdown had waned or in recruited $CD4^+$ T cells that were not present at the time of knockdown. Although the knockdown of *TREX1* only delayed the progression of HIV infection, but did not inhibit it completely, the suppression of local HIV replication in the genital tract might reduce person-to-person transmission. Future experiments in which *TREX1* AsiCs are administered both before and after HIV challenge should address this question. By measuring viral DNA species and integration of the provirus within different human cell subtypes in the genital tract of humanized mice, we may be able to determine the cell types in which the virus persists during *TREX1* knockdown. The viral setpoint and CD4 depletion in *TREX1* knocked down mice eventually reached the same levels as in mock-treated mice. This surprising finding suggests that the viral setpoint is not determined by the original viral replicative burst, but by the complex interaction of the virus with the host immune system. The conservation of the viral setpoint here may be related to the well-known and poorly understood clinical finding that viral levels return to the pretreatment setpoint when antiretroviral drugs are halted. What determines the viral setpoint in any setting is not well understood.

The in vitro data presented here suggest that there is a narrow temporal window during which IFNs can effectively control infection—the ~30 hr around the time of exposure. Our results echo those found in SIV infection in macaques, in which IFN only effectively blocks infection within a 3-day period (Unterholzner and Bowie, 2008). This may be one of the reasons that chronic IFN therapy showed inconsistent results in clinical trials and ultimately did not appreciably improve patient outcomes (Fitzgerald-Bocarsly and Jacobs, 2010; Jackson et al., 2006; Lehmann et al., 2010; Saba et al., 2010; Swiecki and Colonna, 2010). In addition to timing, location also seems to play a critical role. IFNs at the site of transmission provided protection, but after systemic IFN treatment, protection was lost, likely due to a shift in balance between protective and harmful IFN-triggered downstream events. Our finding in humanized mice differs from results in macaques, where i.v. PEGylated-IFN, begun before SIV challenge and continued for 4 weeks, provided protection from rectal challenge (Unterholzner and Bowie, 2008). Multiple variables could account for these differing observations including differences between species, site of infection, virus, and dose and type of rIFN.

This study uses in vivo gene knockdown as a tool to explore the earliest stages of HIV disease pathogenesis and the role IFNs play in transmission. Knockdown of individual host genes in all the cells that HIV infects using CD4-AsiCs provides a straightforward method to explore the role of individual host genes in HIV transmission. Preliminary results suggest that the CD4-aptamer also recognizes macaque CD4 (data not shown). Thus, this tool could also be used to study the role of host genes in SIV transmission in macaques, where gene knockout is not easy. We have recently found that EpCAM-AsiCs given subcutaneously can silence gene expression in EpCAM+ cells distributed at distal sites throughout the mouse (Gilboa-Geffen et al., 2015). Preliminary studies of subcutaneous injection of CD4-AsiCs in humanized mice also show strong knockdown (~80%) in $CD4^+$ T cells in local lymph nodes, as well as in the

RNA by qRT-PCR (left), plasma HIV p24-Ag by ELISA (middle), and circulating $CD4^+$ T cell count by flow cytometry (right). The dashed line represents the threshold of detection of the assay. No CD4 analysis was performed at week 4.

(E) shows average ± SEM for each group. *$p < 0.05$; ***$p < 0.005$, ***$p < 0.0005$, by one-way ANOVA, relative to PBS control. The graphs represent data from one of two independent experiments with different batches of BLT mice prepared with human hematopoietic stem cells from two different donors.

spleen and distal lymph nodes. These findings suggest that this powerful tool could be used to study the influence of individual host genes not only on transmission, but also on disease progression and pathogenesis.

EXPERIMENTAL PROCEDURES

CD4-AsiC Synthesis

CD4-AsiCs were synthesized using the primer sequences given in Table S1 using in vitro transcription as described (Davis et al., 1998; McNamara et al., 2006; Wheeler et al., 2011). Sequences for the conjugated siRNAs are shown in Table S2.

Human Cervical Polarized Tissue Explants

Human cervical tissue was obtained with Boston Children's Hospital (BCH) and Harvard Medical School (HMS) Human Investigational Review Board approval from healthy donors undergoing hysterectomy for benign conditions and was prepared as previously described (Wheeler et al., 2011, 2013).

BLT Mouse Experiments

Animal work was approved by the Animal Care and Use Committees of Massachusetts General Hospital, BCH and HMS. All in vivo experiments were performed using progesterone-treated, ketamine/xylazine anesthetized NOD/SCID/*IL2rg*$^{-/-}$ (NSG) female mice, bearing humanized bone marrow following reconstitution with CD34^{+} cells from human fetal liver and surgical human thymic grafts (BLT mice), prepared by the MGH Humanized Mouse Program as previously described (Brainard et al., 2009; Kumar et al., 2008; Wheeler et al., 2011, 2013). Uniform HIV infection in challenge experiments was obtained by requiring high levels of human immune reconstitution using previously described criteria (Wheeler et al., 2011, 2013). These criteria included a minimum of 25% of human CD45^{+} cells in the blood, of which at least 50% are lymphocytes (and at least 40% of these are T cells). The absolute number of human T cells was required to be at least 200/100 μl of blood. BLT mice were treated with PBS or 80 pmol of CD4-AsiCs in PBS by atraumatic application to the vaginal mucosa in 15 μl according to the indicated schedule. For infections, $HIV_{JR\text{-}CSF}$ (10^5 $TCID_{50}$) diluted in 10 μl PBS was applied atraumatically to the vaginal mucosa. Mice were kept supine for 5 min after each application. For some experiments 1 μg/ml of LPS (List Biological Laboratories) was applied IVAG. For other experiments, rIFN (R&D Systems) was administered either by tail vein injection (10,000 IU in 50 μl PBS) or by IVAG administration (2,000 IU in 10 μl PBS). For all post-treatment analysis, both the vaginal tissue and peripheral blood were harvested and processed as previously described (Wheeler et al., 2011, 2013). Single cell suspensions were stained using 1/100 dilutions of hCD45 and hCD4 antibodies (BioLegend) and sorted by FACS for gene expression analysis.

Additional experimental methods are described in the Supplemental Experimental Procedures.

SUPPLEMENTAL INFORMATION

Supplemental Information includes Supplemental Experimental Procedures, five figures, and three tables and can be found with this article online at http://dx.doi.org/10.1016/j.celrep.2016.04.048.

AUTHOR CONTRIBUTIONS

J.L., L.A.W., and R.T. designed the research plan and wrote the manuscript. L.A.W. and R.T. performed experiments with assistance of V.V., N.B., X.L., B.B., L.O., S.M., and S.R. A.D.L. and A.M.T. supervised and helped design the humanized mouse experiments.

ACKNOWLEDGMENTS

This work was supported by grants from the NIH (AI102816 and AI090671 to J.L.; AI078897 to A.M.T. and A.D.L.), the Harvard CFAR (AI060354 to A.M.T. and A.D.L.), the Ragon Institute (to J.L., A.M.T., and A.D.L.), and fellowships from the Cancer Research Institute, the Adelstein Fund, the Harvard Medical School MD/PhD Program and the Point Foundation (to L.A.W.), and the Harvard CFAR (P30 AI060354 to R.T.). We thank T. Allen and T. Dudek and the Virology Core of the Ragon Institute for providing viral stocks for in vivo studies and E. Oliva, M. Miri, and A. Bodo, MGH Surgical Pathology, and L. Yang, BIDMC, for tissue specimens.

Received: November 3, 2015
Revised: March 21, 2016
Accepted: April 9, 2016
Published: May 12, 2016

REFERENCES

Agy, M.B., Acker, R.L., Sherbert, C.H., and Katze, M.G. (1995). Interferon treatment inhibits virus replication in HIV-1- and SIV-infected CD4+ T-cell lines by distinct mechanisms: evidence for decreased stability and aberrant processing of HIV-1 proteins. Virology *214*, 379–386.

Arfi, V., Rivière, L., Jarrosson-Wuillème, L., Goujon, C., Rigal, D., Darlix, J.L., and Cimarelli, A. (2008). Characterization of the early steps of infection of primary blood monocytes by human immunodeficiency virus type 1. J. Virol. *82*, 6557–6565.

Bergamaschi, A., and Pancino, G. (2010). Host hindrance to HIV-1 replication in monocytes and macrophages. Retrovirology *7*, 31.

Boasso, A., Hardy, A.W., Anderson, S.A., Dolan, M.J., and Shearer, G.M. (2008). HIV-induced type I interferon and tryptophan catabolism drive T cell dysfunction despite phenotypic activation. PLoS ONE *3*, e2961.

Brainard, D.M., Seung, E., Frahm, N., Cariappa, A., Bailey, C.C., Hart, W.K., Shin, H.S., Brooks, S.F., Knight, H.L., Eichbaum, Q., et al. (2009). Induction of robust cellular and humoral virus-specific adaptive immune responses in human immunodeficiency virus-infected humanized BLT mice. J. Virol. *83*, 7305–7321.

Cai, X., Chiu, Y.H., and Chen, Z.J. (2014). The cGAS-cGAMP-STING pathway of cytosolic DNA sensing and signaling. Mol. Cell *54*, 289–296.

Caux, C., Ait-Yahia, S., Chemin, K., de Bouteiller, O., Dieu-Nosjean, M.C., Homey, B., Massacrier, C., Vanbervliet, B., Zlotnik, A., and Vicari, A. (2000). Dendritic cell biology and regulation of dendritic cell trafficking by chemokines. Springer Semin. Immunopathol. *22*, 345–369.

Coccia, E.M., Krust, B., and Hovanessian, A.G. (1994). Specific inhibition of viral protein synthesis in HIV-infected cells in response to interferon treatment. J. Biol. Chem. *269*, 23087–23094.

Collins, K.B., Patterson, B.K., Naus, G.J., Landers, D.V., and Gupta, P. (2000). Development of an in vitro organ culture model to study transmission of HIV-1 in the female genital tract. Nat. Med. *6*, 475–479.

d'Ettorre, G., Ceccarelli, G., Giustini, N., Mastroianni, C.M., Silvestri, G., and Vullo, V. (2014). Taming HIV-related inflammation with physical activity: a matter of timing. AIDS Res. Hum. Retroviruses *30*, 936–944.

Davis, K.A., Lin, Y., Abrams, B., and Jayasena, S.D. (1998). Staining of cell surface human CD4 with 2′-F-pyrimidine-containing RNA aptamers for flow cytometry. Nucleic Acids Res. *26*, 3915–3924.

Dieu-Nosjean, M.C., Vicari, A., Lebecque, S., and Caux, C. (1999). Regulation of dendritic cell trafficking: a process that involves the participation of selective chemokines. J. Leukoc. Biol. *66*, 252–262.

Fitzgerald-Bocarsly, P., and Jacobs, E.S. (2010). Plasmacytoid dendritic cells in HIV infection: striking a delicate balance. J. Leukoc. Biol. *87*, 609–620.

Gao, D., Wu, J., Wu, Y.T., Du, F., Aroh, C., Yan, N., Sun, L., and Chen, Z.J. (2013). Cyclic GMP-AMP synthase is an innate immune sensor of HIV and other retroviruses. Science *341*, 903–906.

Gilboa-Geffen, A., Hamar, P., Le, M.T.N., Wheeler, L.A., Trifonova, R., Petrocca, F., Wittrup, A., and Lieberman, J. (2015). Gene Knockdown by EpCAM Aptamer-siRNA Chimeras Suppresses Epithelial Breast Cancers and Their Tumor-Initiating Cells. Mol. Cancer Ther. *14*, 2279–2291.

Goldfeld, A.E., Birch-Limberger, K., Schooley, R.T., and Walker, B.D. (1991). HIV-1 infection does not induce tumor necrosis factor-alpha or interferon-beta gene transcription. J. Acquir. Immune Defic. Syndr. *4*, 41–47.

Haase, A.T. (2010). Targeting early infection to prevent HIV-1 mucosal transmission. Nature *464*, 217–223.

Hansen, K., Prabakaran, T., Laustsen, A., Jørgensen, S.E., Rahbæk, S.H., Jensen, S.B., Nielsen, R., Leber, J.H., Decker, T., Horan, K.A., et al. (2014). Listeria monocytogenes induces IFNβ expression through an IFI16-, cGAS- and STING-dependent pathway. EMBO J. *33*, 1654–1666.

Hardy, G.A., Sieg, S.F., Rodriguez, B., Jiang, W., Asaad, R., Lederman, M.M., and Harding, C.V. (2009). Desensitization to type I interferon in HIV-1 infection correlates with markers of immune activation and disease progression. Blood *113*, 5497–5505.

Hasan, M., Koch, J., Rakheja, D., Pattnaik, A.K., Brugarolas, J., Dozmorov, I., Levine, B., Wakeland, E.K., Lee-Kirsch, M.A., and Yan, N. (2013). Trex1 regulates lysosomal biogenesis and interferon-independent activation of antiviral genes. Nat. Immunol. *14*, 61–71.

Hübner, W., Chen, P., Del Portillo, A., Liu, Y., Gordon, R.E., and Chen, B.K. (2007). Sequence of human immunodeficiency virus type 1 (HIV-1) Gag localization and oligomerization monitored with live confocal imaging of a replication-competent, fluorescently tagged HIV-1. J. Virol. *81*, 12596–12607.

Jackson, A.L., Burchard, J., Leake, D., Reynolds, A., Schelter, J., Guo, J., Johnson, J.M., Lim, L., Karpilow, J., Nichols, K., et al. (2006). Position-specific chemical modification of siRNAs reduces "off-target" transcript silencing. RNA *12*, 1197–1205.

Judge, A.D., Sood, V., Shaw, J.R., Fang, D., McClintock, K., and MacLachlan, I. (2005). Sequence-dependent stimulation of the mammalian innate immune response by synthetic siRNA. Nat. Biotechnol. *23*, 457–462.

Klatt, N.R., Bosinger, S.E., Peck, M., Richert-Spuhler, L.E., Heigele, A., Gile, J.P., Patel, N., Taaffe, J., Julg, B., Camerini, D., et al. (2014). Limited HIV infection of central memory and stem cell memory CD4+ T cells is associated with lack of progression in viremic individuals. PLoS Pathog. *10*, e1004345.

Kumar, P., Ban, H.S., Kim, S.S., Wu, H., Pearson, T., Greiner, D.L., Laouar, A., Yao, J., Haridas, V., Habiro, K., et al. (2008). T cell-specific siRNA delivery suppresses HIV-1 infection in humanized mice. Cell *134*, 577–586.

Kumar, A., Abbas, W., and Herbein, G. (2014). HIV-1 latency in monocytes/macrophages. Viruses *6*, 1837–1860.

Lahaye, X., Satoh, T., Gentili, M., Cerboni, S., Conrad, C., Hurbain, I., El Marjou, A., Lacabaratz, C., Lelièvre, J.D., and Manel, N. (2013). The capsids of HIV-1 and HIV-2 determine immune detection of the viral cDNA by the innate sensor cGAS in dendritic cells. Immunity *39*, 1132–1142.

Lehmann, C., Lafferty, M., Garzino-Demo, A., Jung, N., Hartmann, P., Fätkenheuer, G., Wolf, J.S., van Lunzen, J., and Romerio, F. (2010). Plasmacytoid dendritic cells accumulate and secrete interferon alpha in lymph nodes of HIV-1 patients. PLoS ONE *5*, e11110.

McNamara, J.O., 2nd, Andrechek, E.R., Wang, Y., Viles, K.D., Rempel, R.E., Gilboa, E., Sullenger, B.A., and Giangrande, P.H. (2006). Cell type-specific delivery of siRNAs with aptamer-siRNA chimeras. Nat. Biotechnol. *24*, 1005–1015.

Miller, C.J., Li, Q., Abel, K., Kim, E.Y., Ma, Z.M., Wietgrefe, S., La Franco-Scheuch, L., Compton, L., Duan, L., Shore, M.D., et al. (2005). Propagation and dissemination of infection after vaginal transmission of simian immunodeficiency virus. J. Virol. *79*, 9217–9227.

Monroe, K.M., Yang, Z., Johnson, J.R., Geng, X., Doitsh, G., Krogan, N.J., and Greene, W.C. (2014). IFI16 DNA sensor is required for death of lymphoid CD4 T cells abortively infected with HIV. Science *343*, 428–432.

Olesen, R., Wahl, A., Denton, P.W., and Garcia, J.V. (2011). Immune reconstitution of the female reproductive tract of humanized BLT mice and their susceptibility to human immunodeficiency virus infection. J. Reprod. Immunol. *88*, 195–203.

Orzalli, M.H., Broekema, N.M., Diner, B.A., Hancks, D.C., Elde, N.C., Cristea, I.M., and Knipe, D.M. (2015). cGAS-mediated stabilization of IFI16 promotes innate signaling during herpes simplex virus infection. Proc. Natl. Acad. Sci. USA *112*, E1773–E1781.

Parrish, N.F., Gao, F., Li, H., Giorgi, E.E., Barbian, H.J., Parrish, E.H., Zajic, L., Iyer, S.S., Decker, J.M., Kumar, A., et al. (2013). Phenotypic properties of transmitted founder HIV-1. Proc. Natl. Acad. Sci. USA *110*, 6626–6633.

Piguet, V., and Steinman, R.M. (2007). The interaction of HIV with dendritic cells: outcomes and pathways. Trends Immunol. *28*, 503–510.

Poli, G., Biswas, P., and Fauci, A.S. (1994). Interferons in the pathogenesis and treatment of human immunodeficiency virus infection. Antiviral Res. *24*, 221–233.

Rasaiyaah, J., Tan, C.P., Fletcher, A.J., Price, A.J., Blondeau, C., Hilditch, L., Jacques, D.A., Selwood, D.L., James, L.C., Noursadeghi, M., and Towers, G.J. (2013). HIV-1 evades innate immune recognition through specific cofactor recruitment. Nature *503*, 402–405.

Saba, E., Grivel, J.C., Vanpouille, C., Brichacek, B., Fitzgerald, W., Margolis, L., and Lisco, A. (2010). HIV-1 sexual transmission: early events of HIV-1 infection of human cervico-vaginal tissue in an optimized ex vivo model. Mucosal Immunol. *3*, 280–290.

Sandler, N.G., Bosinger, S.E., Estes, J.D., Zhu, R.T., Tharp, G.K., Boritz, E., Levin, D., Wijeyesinghe, S., Makamdop, K.N., del Prete, G.Q., et al. (2014). Type I interferon responses in rhesus macaques prevent SIV infection and slow disease progression. Nature *511*, 601–605.

Shirazi, Y., and Pitha, P.M. (1992). Alpha interferon inhibits early stages of the human immunodeficiency virus type 1 replication cycle. J. Virol. *66*, 1321–1328.

Sun, L., Wu, J., Du, F., Chen, X., and Chen, Z.J. (2013). Cyclic GMP-AMP synthase is a cytosolic DNA sensor that activates the type I interferon pathway. Science *339*, 786–791.

Swiecki, M., and Colonna, M. (2010). Unraveling the functions of plasmacytoid dendritic cells during viral infections, autoimmunity, and tolerance. Immunol. Rev. *234*, 142–162.

Unterholzner, L., and Bowie, A.G. (2008). The interplay between viruses and innate immune signaling: recent insights and therapeutic opportunities. Biochem. Pharmacol. *75*, 589–602.

Wang, Y., Abel, K., Lantz, K., Krieg, A.M., McChesney, M.B., and Miller, C.J. (2005). The Toll-like receptor 7 (TLR7) agonist, imiquimod, and the TLR9 agonist, CpG ODN, induce antiviral cytokines and chemokines but do not prevent vaginal transmission of simian immunodeficiency virus when applied intravaginally to rhesus macaques. J. Virol. *79*, 14355–14370.

Wheeler, L.A., Trifonova, R., Vrbanac, V., Basar, E., McKernan, S., Xu, Z., Seung, E., Deruaz, M., Dudek, T., Einarsson, J.I., et al. (2011). Inhibition of HIV transmission in human cervicovaginal explants and humanized mice using CD4 aptamer-siRNA chimeras. J. Clin. Invest. *121*, 2401–2412.

Wheeler, L.A., Vrbanac, V., Trifonova, R., Brehm, M.A., Gilboa-Geffen, A., Tanno, S., Greiner, D.L., Luster, A.D., Tager, A.M., and Lieberman, J. (2013). Durable knockdown and protection from HIV transmission in humanized mice treated with gel-formulated CD4 aptamer-siRNA chimeras. Mol. Ther. *21*, 1378–1389.

Wu, L., and KewalRamani, V.N. (2006). Dendritic-cell interactions with HIV: infection and viral dissemination. Nat. Rev. Immunol. *6*, 859–868.

Yan, N., Cherepanov, P., Daigle, J.E., Engelman, A., and Lieberman, J. (2009). The SET complex acts as a barrier to autointegration of HIV-1. PLoS Pathog. *5*, e1000327.

Yan, N., Regalado-Magdos, A.D., Stiggelbout, B., Lee-Kirsch, M.A., and Lieberman, J. (2010). The cytosolic exonuclease TREX1 inhibits the innate immune response to human immunodeficiency virus type 1. Nat. Immunol. *11*, 1005–1013.

Zhang, Z., Schuler, T., Zupancic, M., Wietgrefe, S., Staskus, K.A., Reimann, K.A., Reinhart, T.A., Rogan, M., Cavert, W., Miller, C.J., et al. (1999). Sexual transmission and propagation of SIV and HIV in resting and activated CD4+ T cells. Science *286*, 1353–1357.

Zhang, R., Bloch, N., Nguyen, L.A., Kim, B., and Landau, N.R. (2014). SAMHD1 restricts HIV-1 replication and regulates interferon production in mouse myeloid cells. PLoS ONE *9*, e89558.

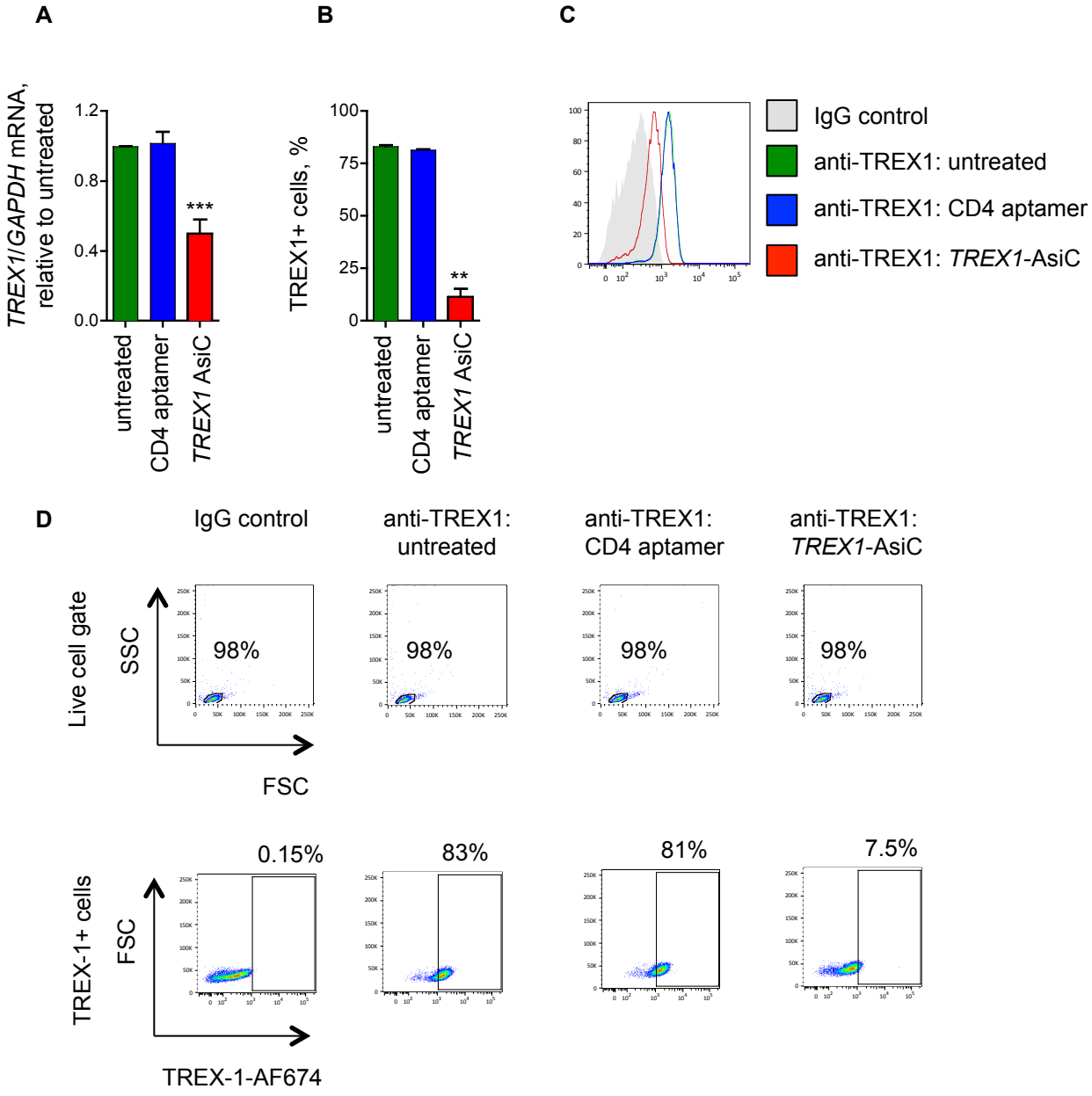

Figure S1. Related to Figure 1: Knockdown of *TREX1* after treatment with *TREX1* CD4-AsiCs.
Expression of *TREX1* mRNA in human primary CD4+ T cells was measured by qRT-PCR relative to *GAPDH* (**A**) and of TREX1 protein was measured by intracellular staining and flow cytometry (**B-D**) 3 d and 7 d, respectively, after treatment with 2 µM *TREX1* AsiC or CD4 aptamer. (**, p< 0.01, ***, p< 0.001). Data are normalized to untreated control and represent mean + S.E.M.

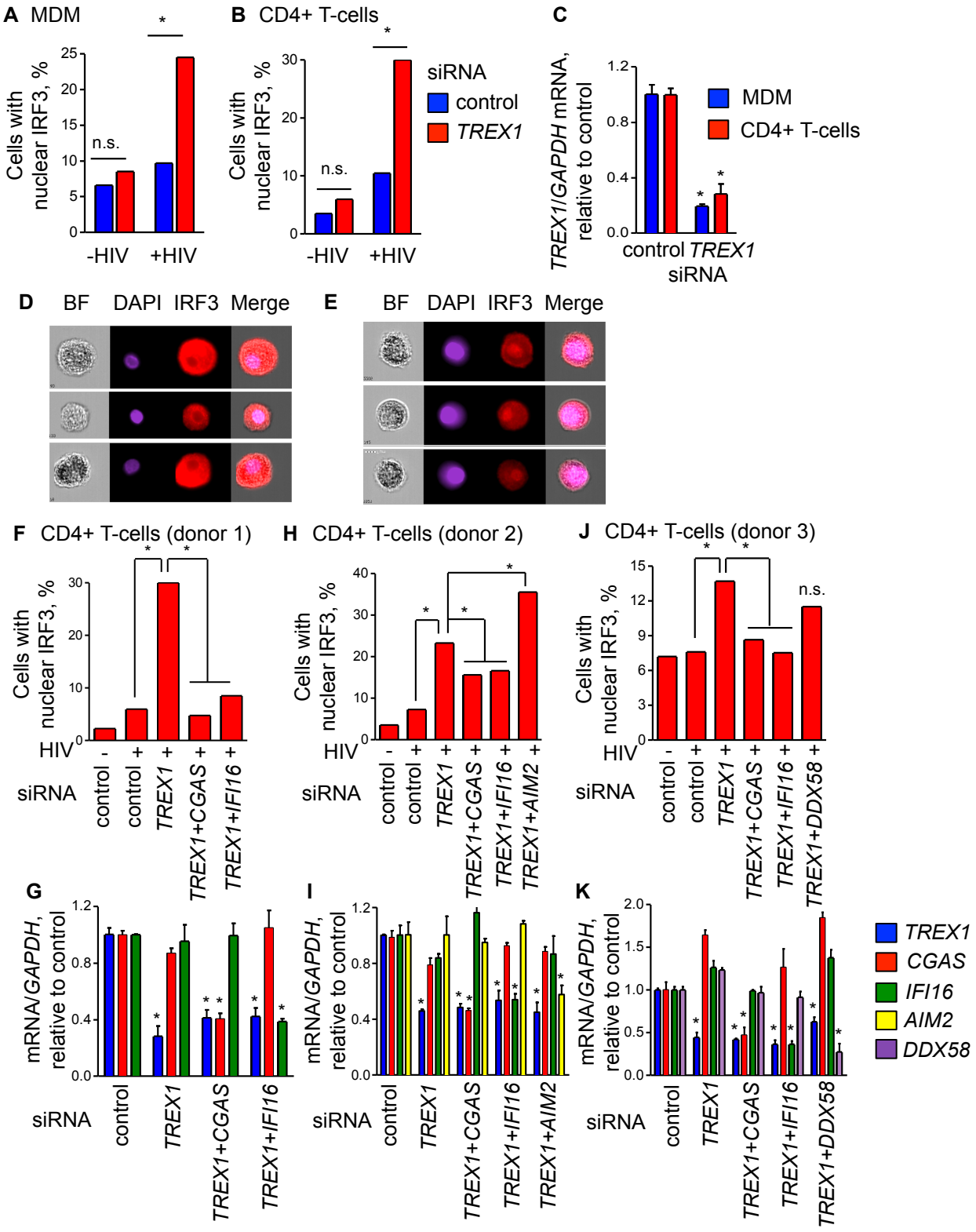

Figure S2. Related to Figure 2: IRF3 nuclear translocation in HIV-infected cells after *TREX1* knockdown.
Nuclear translocation of IRF3 was measured by imaging cytometry performed 16 hrs after HIV infection in primary human MDM (**A**) and CD4+ T-cells (**B**) previously transfected with siRNAs targeting *TREX1* or with non-targeting negative control siRNA. Shown are representative images of MDMs without (**D**) or with (**E**) nuclear IRF3 (BF, brightfield; DAPI, nuclear stain). (**F, H, J**) Nuclear translocation of IRF3 16 hr after HIV infection of primary human CD4+ T cells transfected with siRNAs targeting *TREX1* alone or together with *CGAS*, *IFI16, AIM2 or DDX58*, the gene encoding RIG-I. The data were obtained with PBMCs from three healthy donors and at least 5,000 events were analyzed for each condition. Knockdown was confirmed by qRT-PCR 2 d post transfection (**C** for data in A and B; **G, I, K** for data in F, H and J, respectively). P values in (C,G,I,K) were calculated by Student's t-test (*, $p < 0.001$ compared to control). P values in (A,B,F,H,J) were calculated by Chi–squared test (*, $p < 0.001$, n.s., not significant).

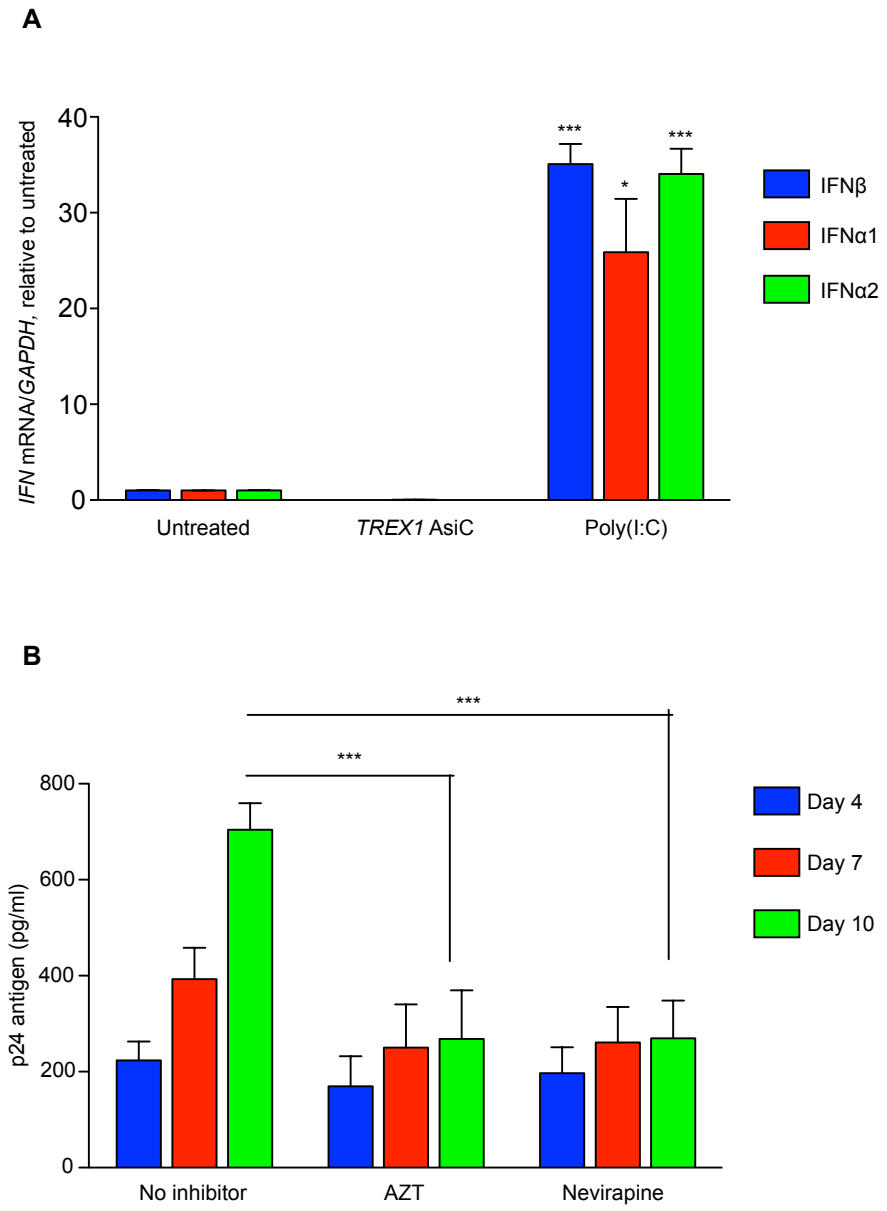

Figure S3. Related to Figure 2: Interferon response after treatment with *TREX1* AsiCs and HIV replication in polarized human cervical explants.

(A) Lack of IFN induction in human cervical explants treated with *TREX1* AsiC alone. Type I IFN mRNAs were measured by qRT-PCR in polarized cervical explants treated for 6 hrs with 4 μM TREX1 AsiCs. Treatment with 100 μg/ml Poly(I:C) was used as a control (*, $p< 0.05$, ***, $p< 0.001$). Data were normalized to *GAPDH* mRNA. Each bar represents mean + S.E.M of cervical explants from a single donor. **(B)** Inhibition of HIV replication in polarized human cervical explants by reverse transcriptase inhibitors. HIV p24 Ag in conditioned media from polarized human cervical explants infected with HIV_{BaL} in the absence or presence of 50 μM Azidothymidine (AZT) or Nevirapine was measured by ELISA. The increasing levels of released p24 that were inhibited by AZT or Nevirapine (***, $p<0.001$) confirm productive HIV infection in human cervical explants. Data represent mean + S.E.M.

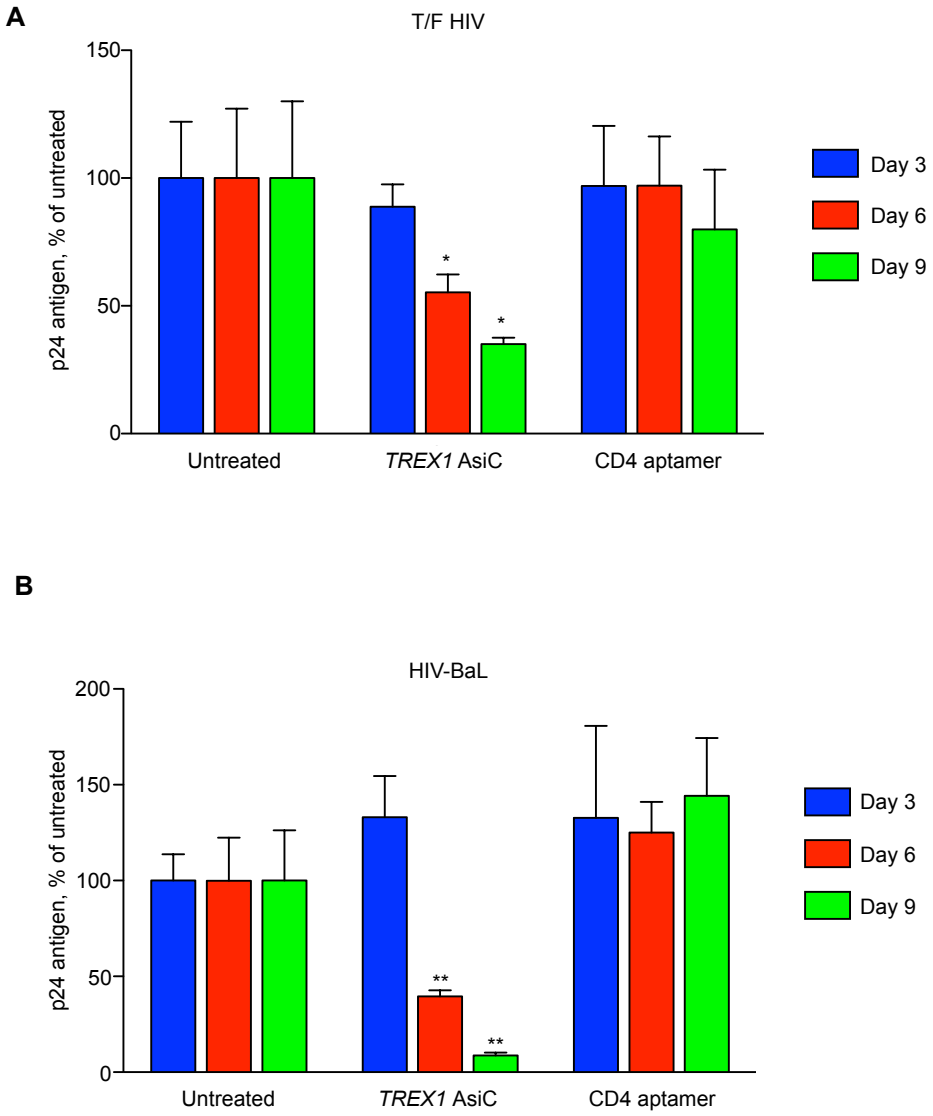

Figure S4. Related to Figure 2: Inhibition of transmitted/founder (T/F) HIV-1 infection in polarized human cervical explants by *TREX1* AsiCs.

HIV p24 Antigen, measured by ELISA, in conditioned media from polarized human cervical explants infected with T/F HIV-1 (pRHPA.c/2635) **(A)** or HIV_{BaL} **(B)** after pre-treatment with 2 μM *TREX1* AsiC or CD4 aptamer 72 and 48 hr prior to infection (*, $p< 0.05$, **, $p< 0.01$). Data represent mean + S.E.M, normalized to the untreated sample on the same day.

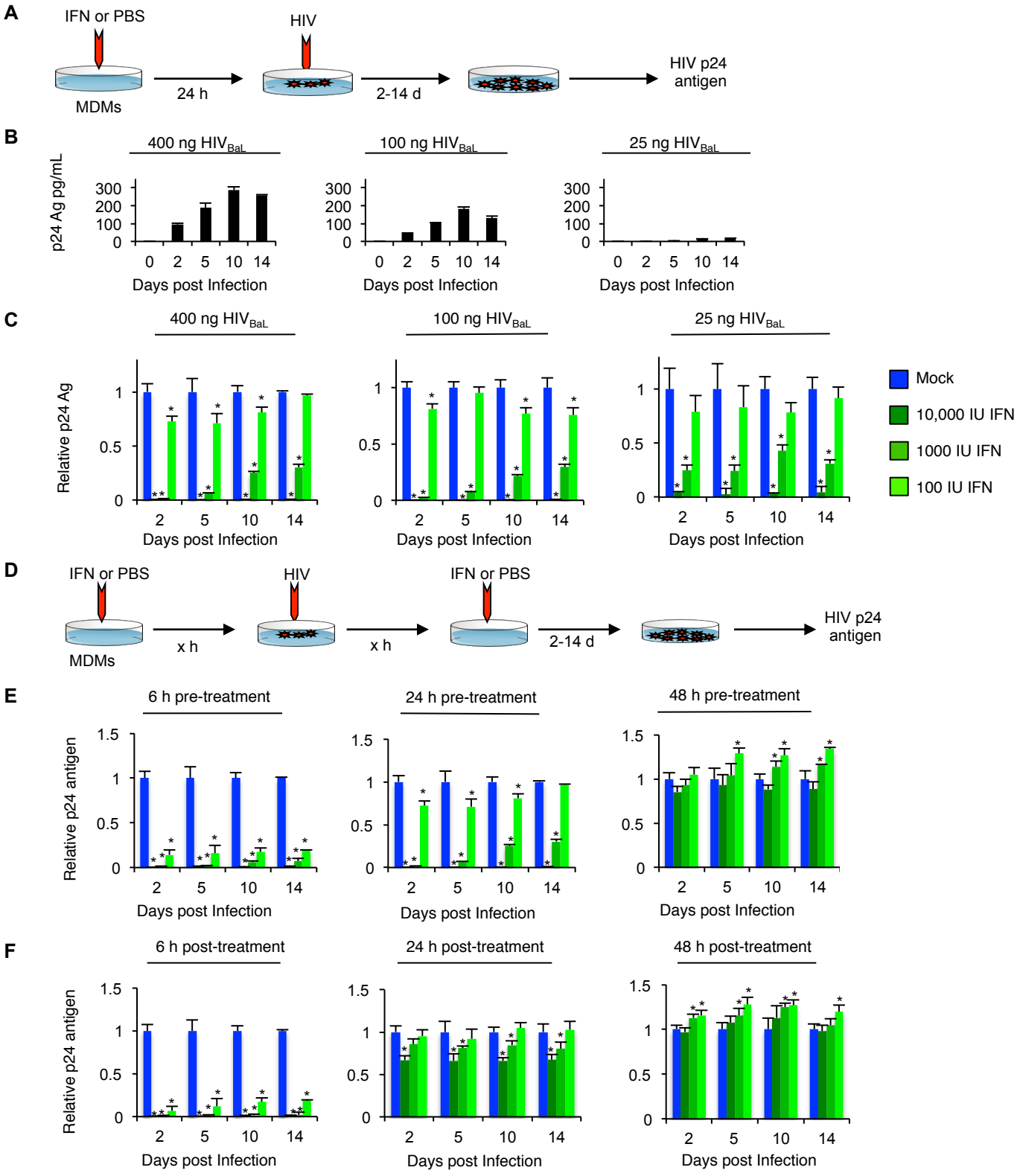

Figure S5. Related to Figure 3 and 4: Treatment with rIFN protects patient-derived MDMs from HIV infection when administered between 24 h prior to infection and 6 h after infection. (A-C) Experimental schema **(A)** MDMs derived from two healthy donors were pretreated with PBS or rIFN at indicated doses and challenged 24 h later with indicated concentrations of HIV$_{BaL}$. HIV infection was analyzed by p24 Ag ELISA of culture supernatants. (**B**) shows the time course of infection without IFN pretreatment and **(C)** shows the relative p24 Ag produced at each timepoint, corrected for background in uninfected samples and normalized to cultures that did not receive rIFN (mock, blue). **(D-F)** Experimental schema as above, except that rIFN was added to cultures at indicated times before (**E**) and after (**F**) HIV challenge. p24 Ag in culture supernatants was normalized to mock cultures that were infected, but did not receive rIFN. All graphs show mean + SEM of 3 independent experiments (*p <0.05, relative to mock-treated sample, by Student's t-test).

Table S1: Primers for AsiC Synthesis

5' Primers	
5' T7 Primer CD4	5' - TAA TAC GAC TCA CTA TAG GGA GAC AAG AAT AAA CGC - 3'
Template DNA	
CD4 Aptamer	5' - GGG AGA CAA GAA TAA ACG CTC AAT GAC GTC CTT AGA ATT GCG CAT TCC TCA CAC AGG ATC TTT TCG ACA GGA GGC TCA CAA CAG GC - 3'
3' Primers	
3' *TREX* Primer "Sequence a"	5' – TCG TAG CGG TCA CCA TTG TGC CTG TTG TGA GCC TCC TGT CGA A - 3'
3' *TREX* Primer "Sequence b"	5' – TGA CAG CAG ATG GTC TTG GGC CTG TTG TGA GCC TCC TGT CGA A - 3'
3' *CCR5* Primer CD4	5' - AAT TTC GAC ACC GAA GCA GAG GCC TGT TGT GAG CCT CCT GTC GAA - 3'
3' *gag* Primer CD4	5' - AAC CTG TCT CTC AGT ACA ATC GCC TGT TGT GAG CCT CCT GTC GAA - 3'
3' *vif* Primer CD4	5' - AAG GGA TGT GTA CTT CTG AAC GCC TGT TGT GAG CCT CCT GTC GAA - 3'

Table S2: siRNAs

CCR5	Sense: 5’ P-CUC UGC UUC GGU GUC GAA A dTdT - 3'
	Antisense: 5’ P-UUU CGA CAC CGA AGC AGA G dTdT - 3’
gag	Sense: 5' P-GAU UGU ACU GAG AGA CAG GCU-dTdT – 3’
	Antisense: 5' P-CCU GUC UCU CUC AGU ACA AUC dTdT-3'
vif	Sense: 5' P-GTT CAG AAG TAC ACA TCC C-dTdT
	Antisense: 5' P-GGG AUG UGU ACU UCU GAA CdTdT-3'
TREX1 Sequence a	Sense: 5’ P- ACA AUG GUG ACC GCU ACG AdTdT -3’
	Antisense: 5’ P-TCG TAG CGG TCA CCA TTG TdTdT -3’
TREX1 Sequence a	Sense: 5’ P- ACA AUG GUG ACC GCU ACG AdTdT -3’
	Antisense: 5’ P-TCG TAG CGG TCA CCA TTG TdTdT -3’

Table S3: Primers for RT-PCR

GAPDH For	5' - AGC CAC ATC GCT CAG ACA C - 3'
GAPDH Rev	5' - GCC CAA TAC GAC CAA ATC C - 3'
IL-8 For	5' - AGA CAG CAG AGC ACA CAA GC - 3'
IL-8 Rev	5' - ATG GTT CCT TCC GGT GGT - 3'
IL-6 For	5' - GAT GAG TAC AAA AGT CCT GAT CCA - 3'
IL-6 Rev	5' - CTG CAG CCA CTG GTT CTG T - 3'
IFNα For	5' – GCT TTA CTG ATG GTC CTG GTG GTG – 3'
IFNα Rev	5' – GAG ATT CTG CTC ATT TGT GCC AG - 3'
IFNβ For	5' - TTG CTC TGG CAC AAC AGG TA - 3'
IFNβ Rev	5' - TGG AGA AGC AAC CAG GAG A - 3'
IFNγ For	5' - GGC ATT TTG AAG AAT TGG AAA G - 3'
IFNγ Rev	5' - TTT GGA TGC TCT GGT CAT CTT - 3'
OAS-1 For	5' - GGT GGA GTT CGA TGT GCT G - 3'
OAS-1 Rev	5' - AGG TTT ATA GCC GCC AGT CA - 3'
IP-10 For	5' - GAA AGC AGT TAG CAA GGA AAG GT - 3'
IP-10 Rev	5' - GAC ATA TAC TCC ATG TAG GGA AGT GA - 3'
STAT1 For	5' - TTG GCA CCT AAC GTG CTG - 3'
STAT1 Rev	5' - TTC GTA CCA CTG AGA CAT CCT G - 3'
IL-12 For	5' - CAC TCC CAA AAC CTG CTG CTG AG - 3'
IL-12 Rev	5' - TCT CTT CAG AAG TGC AAG GGT A - 3'
HIV-gag For	5' – AGT GGG GGG ACA TCA AGC AGC CAT GCA AAT – 3'
HIV-gag Rev	5' – TGC TAT GTC ACT TCC CCT TGG TTC TCT – 3'
TREX1 For	5' – GCA TCT GTC AGT GGA GAC CA – 3'
TREX1 Rev	5' – AGA TCC TTG GTA CCC CTG CT – 3'
IL1-β For	5' – GTG AAA TGA TGG CTT ATT ACA GTG – 3'
IL1-β Rev	5' – CTG ACG CGG CCT GCC TGA AGC CCT – 3'
TNFα For/Rev	IDT Prime Time Primer Sequence Hs.PT.58.45380900
CCR5 For/Rev	IDT Prime Time Primer Sequence Hs.PT.58.3437570
cGAS For	5' – GGG AGC CCT GCT GTA ACA CTT CTT AT – 3'
cGAS Rev	5' – CCT TTG CAT GCT TGG GTA CAA GGT – 3'
IFI16 For	5' – GGT CTG CGA TCC TGA ATG GG – 3'
IFI16 Rev	5' – TCA CTA TCG AGA TAC TTG TGG GT – 3'
AIM2 For	5' – TGG CAA AAC GTC TTC AGG AGG– 3'
AIM2 Rev	5' – AGC TTG ACT TAG TGG CTT TGG– 3'
DDX58 For	5' – GTG CAA AGC CTT GGC ATG T – 3'
DDX58 Rev	5' – TGG CTT GGG ATG TGG TCT ACT C – 3'

Supplemental Experimental Procedures

Cells. Human PBMCs were isolated by Ficoll (GE) density centrifugation from whole blood obtained from the Kraft Family Blood Donor Center and from the Brigham and Women's Hospital Specimen Bank, Boston, MA with Institutional Review Board approval. Mononuclear cells were cultured in H10 medium (RPMI 1640 (Cellgro) containing 10% Human AB serum (GemCell), 100 U/mL penicillin and 100 µg /mL streptomycin sulfate). CD4+ cells were separated using immunomagnetic beads (Miltenyi) and CD4+ T cells and MDMs were prepared as previously described (Song et al., 2003). T cells were cultured in H10 containing 60 IU/mL IL-2 (Proleukin from Chiron Corporation, Emeryville, CA) and were activated using 4 µg/mL PHA (Difco). Resting PBMCs were cultured in H10 containing 4 µg/mL IL-15 (R&D Systems).

Quantitative RT-PCR (qRT-PCR) was performed as previously described (Palliser et al., 2006) using primers in **Table S3**. mRNA expression was normalized to *GAPDH* expression, and then calculated as a percentage relative to mock-treated controls.

Flow cytometry. Direct immunostaining of CD3, CD4, CD8, CD14, CD45, and CD19 was performed using 1/20 dilutions of fluorescently conjugated murine mAb (BioLegend) for 30-60 min at 4 ºC. Cells were stained in PBS containing 0.5% FCS, 1 mM EDTA, and 25 mM HEPES. Samples were washed twice in the same buffer. Intracellular flow cytometry for TREX1 was performed using a rabbit monoclonal antibody (Abcam, Cambridge, MA) with a donkey anti-rabbit AF647 secondary antibody (Life Technologies). Data were acquired for one and two-color experiments using a FACSCalibur (BD Biosciences), and for multi-color and cell sorting experiments using a FACSAria II (BD Biosciences). All data were analyzed using FlowJo (Treestar, Inc.) software.

Viruses. HIV_{BaL} was used to infect cells and cervicovaginal explants *in vitro* unless otherwise specified. HIV_{IIIB} was used to infect primary CD4+ T cells. HIV_{BaL} and HIV_{IIIB} were obtained from the NIH AIDS Research and Reference Reagent Program and viral stocks were generated as previously described (Wheeler et al., 2011; Wheeler et al., 2013). For mouse experiments $HIV\text{-}1_{JR\text{-}CSF}$ stocks were produced by the Virology Core of the Ragon Institute as previously described (Wheeler et al., 2013). T/F HIV-1 Infectious Molecular Clone (pRHPA.c/2635) was obtained from the NIH AIDS Research and Reference Reagent Program, Division of AIDS, NIAID, NIH (cat#11744, from Dr. John Kappes). T/F HIV-1 and HIV_{BaL} (200 µL of $1x10^5$ TCID50/mL virus) were used to infect polarized human cervical explants.

Human cervical polarized tissue explants. AsiCs or aptamers in 50 µL Optimem (Invitrogen) were applied on 2 consecutive days to the apical surface of polarized explants, and the explants were then incubated at 37 °C for 4-6 h before adding 150 µL H10 medium to each well. In some experiments 15 µg of neutralizing antibodies against both IFNα and IFNβ (Cell Sciences and BioLegend, respectively) were added to the culture medium at the same time as the second topical AsiC administration and at the time of HIV infection. At sequential time points, 100 µL of medium from the lower chamber was removed for HIV and IFNβ ELISA assays. Explants were cultured for not more than 10 d to reduce confounding problems due to loss of viability during extended culture. Cervicovaginal tissue was digested with collagenase as previously described (Wheeler et al., 2011; Wheeler et al., 2013). Cell subsets were obtained by fluorescence-activated cell sorting after staining for CD4, CD14, CD3 and CD19. RNA from separated monocyte, CD4 T cell and B cell subsets were analyzed by qRT-PCR.

ELISA assays. p24 antigen levels were measured using the HIV-1 p24 ELISA Kit (Perkin Elmer). IFNβ protein was measured by assay of culture supernatants using the Verikine Human IFN beta ELISA kit (R&D). rhIFN Type I was measured in mouse serum samples using Human IFN-alpha Serum Sample ELISA Kit (R & D Systems).

rIFN. A universal Type I IFN (R&D Systems) was used for both *in vitro* and *in vivo* experiments.

Analysis of HIV infection. Blood was obtained by venipuncture of the facial vein at weekly intervals for 12 wks following HIV challenge. Analysis of HIV infection was as previously described (Wheeler et al., 2011; Wheeler et al., 2013). Cells were pelleted by centrifugation and plasma was stored at -80 ºC until analysis. Cell pellets were twice treated with red blood cell (RBC) lysis buffer (Sigma), washed with flow cytometry buffer described above and stained using a 1/20 dilution of CD3, CD4, and CD8 mAb (BioLegend). Viral RNA was extracted from 75 µL of plasma using Trizol (Invitrogen) according to the manufacturer's instructions. cDNA was reverse transcribed

using SuperscriptIII (Invitrogen) and HIV *gag* mRNA was assessed by qRT-PCR using *gag*-specific primers (**Table S3)**. The remaining serum was aliquoted for p24 Ag ELISA (Perkin Elmer).

Imaging cytometry. MDMs and human primary CD4+ T cells were knocked down for *TREX1, cGAS, IFI16, AIM2, DDX58* as indicated, by siRNA nucleofection as previously described (Yan et al., 2010), and infected 3 days later with HIV_{BaL} and HIV_{IIIB}, respectively. siRNAs targeting *TREX1* were pro-siRNAs produced in bacteria as described (Huang and Lieberman, 2013). siRNAs targeting *cGAS, IFI16, AIM2* and *DDX58* were from Dharmacon (siGENOME™ SMARTpool, except *AIM2* siRNA which were ON-TARGET plus). Non-targeting negative control siRNA was from Ambion (Silencer® Select Negative Control No. 1 siRNA, cat#4390843). Knockdown was confirmed by qRT-PCR 2 d post transfection. Cells were stained 16 hr post infection with DAPI (Sigma) and IRF3 rabbit monoclonal antibody (AbCAM) or rabbit IgG (AbCAM) as control and then donkey anti-rabbit AF647 secondary antibody (Life Technologies) using BD Cytofix/Cytoperm kit (BD Biosciences). Nuclear translocation of IRF3 was assessed using a 5-laser ImageStream X Mark II imaging cytometer (Amnis-Millipore) as described (Fasler-Kan et al, 2016). Cell populations were sequentially gated on single cells positive for DAPI and IRF3 staining. Image analysis was performed using a nuclear mask and Imagestream Data Exploration and Analysis Softare (IDEAS) 6.1 (Amnis-Millipore). The similarity score parameter, a log-transformed Pearson correlation coefficient of the pixel values of two images, was used to correlate the location of IRF3 staining and the nuclear dye (DAPI) to identify cells with nuclear IRF3.

Statistical analysis. Data for most experiments were analyzed by Student's t-test. All P-values are for two-tailed significance tests. For analysis of data based on independent experiments using samples from multiple donors, one-way analysis of variance (ANOVA) with Dunnett multiple comparison test was performed using GraphPad Prism (GraphPad Software). P values for the imaging cytometry experiment were calculated by Chi–squared test. P values below 0.05 were considered significant. The limit of detection of HIV infection was calculated for each assay using the method of (Armbruster and Pry, 2008).

Supplemental References

Armbruster, D.A., and Pry, T. (2008). Limit of blank, limit of detection and limit of quantitation. Clin Biochem Rev *29 Suppl 1*, S49-52.

Fasler-Kan E., Baiken, Y., Vorobjev, I.A., and Barteneva, N.S. (2016). Analysis of nucleocytoplasmic protein shuttling by imaging flow cytometry. In: "Imaging Flow Cytometry: Methods and Protocols" (Eds Barteneva N.S., and Vorobjev, I.A.), Humana Press, pp 127-137.

Huang L. and Lieberman J. (2013). Production of highly potent recombinant siRNAs in Escherichia coli. Nature Protocols 8, 2325–2336.

Palliser, D., Chowdhury, D., Wang, Q.Y., Lee, S.J., Bronson, R.T., Knipe, D.M., and Lieberman, J. (2006). An siRNA-based microbicide protects mice from lethal herpes simplex virus 2 infection. Nature *439*, 89-94.

Song, E., Lee, S.K., Dykxhoorn, D.M., Novina, C., Zhang, D., Crawford, K., Cerny, J., Sharp, P.A., Lieberman, J., Manjunath, N.*, et al.* (2003). Sustained small interfering RNA-mediated human immunodeficiency virus type 1 inhibition in primary macrophages. J Virol *77*, 7174-7181.